**TABLE II. Overall Survival and Disease-Free Survival Rate for Patients of Child-Pugh Class A**

| | Overall survival rate (%) | | | | Disease-free survival rate (%) | | | |
|---|---|---|---|---|---|---|---|---|
| Factor | 1 year | 3 years | 5 years | *P*-value | 1 year | 3 years | 5 years | *P*-value |
| Single HCC >2 cm | | | | 0.57 | | | | 0.048 |
| Resection (n = 72) | 94 | 88 | 83 | | 71 | 43 | 36 | |
| RFA (n = 15) | 100 | 74 | 74 | | 44 | 27 | 9 | |
| Multiple HCC >2 cm | | | | 0.18 | | | | 0.98 |
| Resection (n = 27) | 96 | 96 | 43 | | 60 | 28 | 22 | |
| RFA (n = 5) | 100 | 75 | 38 | | 80 | 0 | 0 | |
| Single HCC ≤2 cm | | | | 0.46 | | | | 0.58 |
| Resection (n = 53) | 100 | 95 | 88 | | 90 | 59 | 53 | |
| RFA (n = 41) | 97 | 94 | 83 | | 81 | 48 | 43 | |
| Multiple HCC ≤2 cm | | | | 0.98 | | | | 0.98 |
| Resection (n = 30) | 92 | 92 | 69 | | 61 | 22 | 22 | |
| RFA (n = 11) | 100 | 92 | 73 | | 80 | 18 | 18 | |

RFA, radiofrequency ablation.

2 cm than for HCC >2 cm; with microvascular invasion (22% vs. 4.3%) and micrometastasis (20.3% vs. 8.3%) being more common in HCCs >2 cm compared to those ≤2 cm.

Ninety-seven (49%) of the patients in the hepatic resection group and 43 (49%) of the patients in the RFA group showed HCC recurrences. The pattern of recurrence and the details of treatments for the recurrences in both groups are shown in Table VI. The main treatment for recurrence was TACE (34%), followed by RFA (28%) and repeat hepatectomy (23%) in the surgical resection group, whereas the main treatment for recurrence was RFA (37%), and followed by TACE (35%) and hepatectomy (16%) in the RFA group. One patient underwent salvage liver transplantation for recurrence in the surgical resection group. The proportion of patients with extrahepatic recurrence tended to be higher in the hepatic resection group ($P = 0.07$), but the modalities of the treatments used for recurrence did not differ among the two groups.

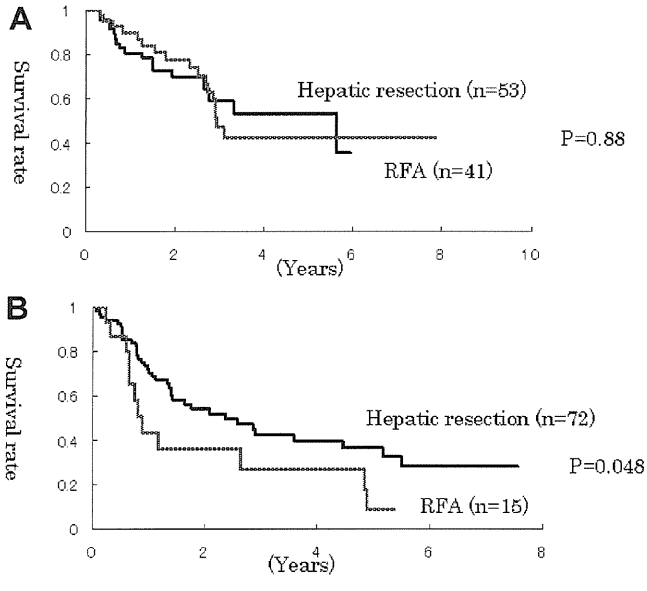


Fig. 2. **A**: Comparison of disease-free survival rates in patients with a single HCC with tumor size less than 2 cm in Child-Pugh A between patients in the surgical resection and RFA groups. **B**: Comparison of disease-free survival rates in patients with a single HCC with tumor size >2 cm in Child-Pugh A between patients in the surgical resection and RFA groups.

## DISCUSSION

Livraghi et al. [7] recently demonstrated that the estimated 3- and 5-year survival rates for the potentially operable subgroup (100 patients with a single HCC ≤2 cm) were 89% and 68%, respectively. They showed that the 5-year survival rate in their study was comparable to that reported by the Liver Cancer Study Group of Japan, which revealed a 5-year survival rate of 70% for 2078 patients. They concluded that RFA can be considered the preferred treatment for patients with single HCC ≤2 cm, even when surgical resection is possible, since RFA is much less invasive and has a lower complication rate, and other approaches can be used as salvage therapy for the few cases in which RFA is unsuccessful or unfeasible. In our study, a combination of TACE and RFA was performed in the majority of patients with hypervascular HCC nodules who did not undergo surgical resection. The diagnosis by CT imaging has the possibility of misdiagnosis of HCC for nodule measuring 2.0 cm or less. Vascular occlusion by TACE permits the formation of larger thermal lesions by reducing heat loss [23,24]. In addition, the accumulation of lipiodol might be useful for obtaining the border of the tumors at CT scan after RFA [19]. In our current study, RFA for HCC smaller than 2 cm has overall and disease-free survival rates similar to those for the resection group. The previous histopathologic studies have shown that, although HCC nodules measuring 1.5 cm or less are uniformly well differentiated, those between 1.5 and 2.0 cm in diameter often contain zones of less differentiated tissue with more intense proliferative activity [25]. Takayama et al. [26] also found that among 70 patients with an early single HCC of 2 cm or less in diameter, only 15 HCC lesions were well-differentiated, and microscopic regional spread (vascular invasion and micrometastasis) was identified in 23 (33%) patients. On the other hand, Wakai et al. [27] shown that vascular invasion was more frequent in patients with HCC >2 cm (16/62, 26%) than in patients with HCC ≤2 cm (1/23, 4%, $P = 0.033$). In the current study, the incidence of micrometastasis and microvascular invasion was significantly lower among patients with HCCs 2 cm or less in diameter than among patients with HCCs larger than 2.0 cm in diameter. Recently, Shi et al. [28] found that among patients with HCCs ≤3 cm, 38 (86%) out of 44 identified micrometastases were located within 1 cm of tumor in the same direction of portal venous, and a resection margin of 1.0 cm is recommended for HCCs ≤3 cm. Theoretically, a single electrode insertion can produce a necrotic area of up to 3.0 cm in diameter, thus allowing full ablation of a 2-cm tumor plus a 0.5–1.0 cm safety margin. Our studies have suggested that the choice of RFA does not matter for patients with single or multiple (less than 3) HCC ≤2 cm, if HCC lesions cannot be visualized by US or are close to anatomic structures that might be damaged by RFA.

**TABLE III. Univariate Analysis of Clinical Factors for Overall Survival and Disease-Free Survival Rate**

| | Overall survival rate (%) | | | | Disease-free survival rate (%) | | | |
|---|---|---|---|---|---|---|---|---|
| Factor | 1 year | 3 years | 5 years | *P*-value | 1 year | 3 years | 5 years | *P*-value |
| Age (year) | | | | 0.53 | | | | 0.7 |
| ≤70 (n = 175) | 97.6 | 89.1 | 76.1 | | 73.1 | 38.4 | 31.7 | |
| >70 (n = 111) | 94.1 | 85.5 | 71.1 | | 72.9 | 39.4 | 27.5 | |
| Gender | | | | 0.15 | | | | 0.8 |
| Male (n = 190) | 96.6 | 86.4 | 72.2 | | 72.4 | 40.4 | 34.4 | |
| Female (n = 96) | 95.6 | 89.9 | 77.3 | | 74.4 | 35.2 | 20.2 | |
| Virus | | | | 0.09 | | | | 0.02 |
| HCV (n = 218) | 96 | 86.3 | 70.9 | | 71.8 | 31.9 | 34.4 | |
| Non-HCV (n = 68) | 96.8 | 89.9 | 84.6 | | 74.4 | 54 | 47.6 | |
| Child-Pugh classification | | | | 0.001 | | | | 0.227 |
| A (n = 254) | 96.6 | 90.7 | 76.6 | | 72.5 | 39.2 | 32.6 | |
| B (n = 32) | 93.5 | 67 | 56.2 | | 74.3 | 34.3 | 10.7 | |
| ICGR 15 (%) | | | | 0.6 | | | | 0.043 |
| <15 (n = 148) | 96.6 | 85.1 | 79 | | 75.1 | 46.9 | 36.9 | |
| ≥15 (n = 137) | 95.6 | 90.4 | 68.9 | | 70.2 | 28.6 | 22.6 | |
| Tumor size (mm) | | | | 0.26 | | | | 0.07 |
| ≤2.0 (n = 157) | 96.4 | 89.8 | 78.7 | | 79.2 | 40.2 | 33.3 | |
| >2.0 (n = 129) | 96 | 85.6 | 69.8 | | 65.1 | 36.2 | 27 | |
| Tumor number | | | | 0.025 | | | | 0.0002 |
| Single (n = 199) | 96.8 | 87.2 | 80.4 | | 75.9 | 45.3 | 36.7 | |
| 2 or 3 (n = 87) | 95 | 88.9 | 59.6 | | 65.1 | 23.9 | 16.6 | |
| DCP (AU/ml) | | | | 0.11 | | | | 0.46 |
| <100 (n = 227) | 97.1 | 89.5 | 76.1 | | 73.1 | 38.7 | 30.5 | |
| ≥100 (n = 59) | 92.8 | 85.6 | 69.3 | | 71.2 | 39.3 | 30.6 | |
| AFP (ng/ml) | | | | 0.65 | | | | 0.64 |
| <100 (n = 215) | 96.5 | 90.2 | 74.8 | | 73 | 38.1 | 30 | |
| ≥100 (n = 71) | 95.5 | 89.4 | 74.9 | | 73.2 | 42.1 | 33.8 | |
| Treatment | | | | 0.11 | | | | 0.88 |
| Resection (n = 199) | 95.6 | 90.9 | 76 | | 71.4 | 41.2 | 33.7 | |
| RFA (n = 87) | 97.6 | 81.4 | 71 | | 76.5 | 34.3 | 24.7 | |

HCV, hepatitis C virus; ICGR 15, indocyanine green retention rate at 15 min; DCP, Des-γ-carboxy prothrombin; AFP, alpha-fetoprotein.

A preliminary report of the Japanese nationwide survey has shown that surgical resection provides a lower time-to-recurrence rate than RFA does among patients with HCCs no more than three tumors (≤3 cm) [12]. In the current study, we have also shown that in subgroup analysis of a single HCC with tumor size >2 cm in Child-Pugh class A, the disease-free survival was longer in the surgical resection group than in the RFA group with significance. The overall survival was longer in the surgical resection group than in the RFA group, although the result was not significant. Our histopathological study has shown that the incidence of micrometastasis was significantly higher among patients with HCCs exceeding 2 cm in diameter (20%) than among patients with HCCs 2.0 cm or less in diameter (8.3%). These findings have suggested that RFA is less effective than hepatic resection to eradicate venous tumor thrombi and micrometastasis in the adjacent liver in addition to the complete removal of the primary HCC with tumor size >2 cm [29,30]. Surgical resection may provide better long-term disease-free survival than RFA in the subgroup of a single HCC exceeding 2 cm of Child-Pugh class A.

We have shown that in subgroup analysis of multiple HCCs exceeding 2 cm in Child-Pugh class A, the overall survival and the disease-free survival in the surgical resection group was not significant different from that in the RFA group. The strategy for multiple HCCs larger than 2 cm in Child-Pugh class A remains unclear because of small sample number in RFA group.

**TABLE IV. Multivariate Analysis of Overall Survival**

| Variable | HR | 95% CI | *P*-value |
|---|---|---|---|
| Child-Pugh class (B vs. A) | 1.669 | 1.016–2.741 | 0.043 |

In our study, Child-Pugh class A and a single tumor were significant favorable prognostic factors for overall survival, and HCV negativity, lower ICGR 15, and a single tumor were significant favorable prognostic factors for disease-free survival in univariate analysis, although in a multivariate study only Child-Pugh class A was an independent favorable factor for overall survival. The preliminary report of the Japanese nationwide survey has shown that in multivariate analysis, low tumor marker, tumor size <2 cm, better liver function (Child-Pugh class A), and the presence of HCV infection were favorable factors for overall survival, and a single tumor, low tumor marker levels, small tumor size, the absence of HCV, and younger age were negative factors for recurrence [12]. These results are similar to trends found in the nationwide study.

Radiofrequency is much less invasive, involves a short hospital stay, and has low mortality associated with the procedure. With the intention of avoiding the risk of hepatic failure that can follow hepatic resection, percutaenous ablation treatments have been proposed due to the efficacy, tolerability, and low risk of the procedure. However, in the

**TABLE V. Pathological Characteristics of HCC of Patients With Hepatic Resection**

| Characteristics | HCC >2 cm (n = 103) | HCC ≤2 cm (n = 96) | *P*-value |
|---|---|---|---|
| Histological type | | | |
| Well/moderate/poor/unknown | 11/75/11/6 | 22/65/4/5 | 0.023 |
| Regional cancer spread | | | |
| Microvascular invasion | 23 (22%) | 4 (4.3%) | 0.0001 |
| Intrahepatic micrometastasis | 21 (20.3%) | 8 (8.3%) | 0.027 |

**TABLE VI. Recurrence and Treatments for Recurrence After Hepatic Resection or RFA**

| | Hepatic resection (n = 199) | RFA (n = 87) | *P*-value |
|---|---|---|---|
| HCC recurrence: yes[a] | 97 (49%) | 43 (49%) | 0.84 |
| Pattern of recurrence[b] | | | 0.07 |
| Intrahepatic | 86 (89%) | 43 (100%) | |
| Intahepatic + extrahepatic | 7 (7%) | 0 (0%) | |
| Extrahepatic | 4 (4%) | 0 (0%) | |
| Treatment: yes[b] | 93 (96%) | 41 (95%) | 0.5 |
| Main modalities[b] | | | 0.67 |
| Hepatectomy | 23 (24%) | 7 (16%) | |
| RFA | 27 (28%) | 16 (37%) | |
| PEI | 3 (3%) | 2 (5%) | |
| TACE | 33 (34%) | 15 (35%) | |
| Liver transplantation | 1 (1%) | 0 (0%) | |
| Others | 6 (6%) | 1 (2%) | |

RFA, radiofrequency ablation; PEI, percutaneous ethanol injection; TACE, transcatheter arterial chemoembolization

[a]Data are expressed as the number of patients (percentage of total patients).

[b]Data are expressed as the number of patients (percentage of patients who had a recurrence).

current study, hepatic resection has been considered as an acceptable treatment, because the procedure-related mortality was zero after hepatectomy, and there was no significant difference in the incidence of morbidity between the two groups, regardless of the high tendency of the incidence of morbidity after hepatic resection.

Our retrospective study had some drawbacks. Clinical characteristics that can strongly influence outcomes differed significantly between the surgical resection group and the RFA group, as shown in other studies. In the current study, the proportion of the multinodular HCC patients and the levels of DCP were higher in the resection group than those in the RFA group, whereas the proportion of poor function liver reserve was lower in the resection group than that in the RFA group. Because multiple nodules and poor function liver reserve are major risks of recurrence, we conducted subgroup analysis according to the tumor size, tumor number, and Child-Pugh class. Ultimately, a randomized controlled trial would be necessary to prospectively determine if RFA and surgery are comparable therapies for early stage HCC.

In conclusion, RFA can be considered the preferred treatment for patients with single or multiple HCC $\leq$2 cm of Child-Pugh class A. Our results suggest that surgical resection may provide better long-term disease-free survival than RFA does in the subgroup of a single HCC exceeding 2 cm of Child-Pugh class A. A large prospective trial comparing surgical resection with RFA is on-going in the Japanese nationwide study, and thus, clear-cut guidelines are expected to be established in the near future.

## REFERENCES


1. Bosh FX, Ribes J, Borras J: Epidemiology of primary liver cancer. Semin Liver Dis 1999;19:271–285.
2. EL-Serag HB, Mason AC: Rising incidence of hepatocellular carcinoma in the United States. N Eng J Med 1999;340:745.
3. Arii S, Yamaoka Y, Futagawa S, et al.: Results of surgical and nonsurgical treatment for small-sized hepatocellular carcinomas: A retrospective and nationwide survey in Japan. Hepatology 2000;32:1224–1229.
4. Livraghi T, Goldberg SN, Lazzaroni S, et al.: Small hepatocellular carcinoma: Treatment with radio-frequency ablation versus ethanol injection. Radiology 1999;210:655–661.
5. Shiina S, Teratani T, Obi S, et al.: A randomized controlled trial of radiofrequency ablation with ethanol injection for small hepatocellular carcinoma. Gastroenterology 2005;129:122–130.
6. Yee W, Lai ECH: The current role of radiofrequency ablation in the management of hepatocellular carcinoma. Ann Surg 2009; 249:20–25.
7. Livraghi T, Meloni F, Di Stasi M, et al.: Sustained complete response and complications rates after radiofrequency ablation of very early hepatocellular carcinoma in cirrhosis: Is resection still the treatment of choice? Hepatology 2008;47: 82–89.
8. Vivarelli M, Guglielmi A, Ruzzenente A, et al.: Surgical resection versus percutaneous radiofrequency ablation in the treatment of hepatocellular carcinoma on cirrhotic liver. Ann Surg 2004;240: 102–107.
9. Hong SN, Lee SY, Choi MS, et al.: Comparing the outcomes of radiofrequency ablation and surgery in patients with a single small hepatocellular carcinoma and well-preserved hepatic function. J Clin Gastroenterol 2005;39:247–252.
10. Chen MS, Li JQ, Zheng Y, et al.: A prospective randomized trial comparing percutaneous local ablation therapy and partial hepatectomy for small hepatocellular carcinoma. Ann Surg 2006; 243:321–328.
11. Guglielmi A, Ruzzenente A, Valdegamberi A, et al.: Radiofrequency ablation versus surgical resection for the treatment of hepatocellular carcinoma in cirrhosis. J Gastrointest Surg 2008; 12:192–198.
12. Hasegawa H, Mukuuchi M, Takayama T, et al.: Surgical resection vs. percutaneous ablation for hepatocellular carcinoma: A preliminary report of the Japanese nationwide survey. J Hepatol 2008;49:589–594.
13. Ueno S, Sakoda M, Kubo F, et al.: Surgical resection versus radiofrequency ablation for small hepatocellular carcinoma within the Milan criteria. J Hepatobiliary Pancreat Surg 2009; 16:359–366.
14. Yamakado K, Nakatsuka A, Takaki H, et al.: Early-stage hepatocellular carcinoma: Radiofrequency ablation combined with chemoembolization versus hepatectomy. Radiology 2008; 247:260–266.
15. Hayashi M, Matsui O, Ueda K, et al.: Progression to hypervascular hepatocellular carcinoma: Correlation with ultranodular blood supply evaluated with CT during injection of contrast material. Radiology 2002;225:143–149.
16. Oishi K, Itamoto T, Kobayashi T, et al.: Hepatectomy for hepatocellular carcinoma in elderly patients aged 75 years or more. J Gastrointest Surg 2009;13:695–701.
17. Itamoto T, Katayama K, Nakahara H, et al.: Autologous blood storage before hepatectomy for hepatocellular carcinoma with underlying liver disease. Br J Surg 2003;90:23–28.
18. Itamoto T, Nakahara H, Amano H, et al.: Repeat hepatectomy for recurrent hepatocellular carcinoma. Surgery 2007;141:589–597.
19. Waki K, Aikata H, Katamura Y, et al.: Percutaneous radiofrequency ablation as a first-line treatment for small hepatocellular carcinoma: Result and prognostic factors on long-term follow-up. J Gastroenterol Hepatol 2010;25:597–604.
20. Dindo D, Demartines N, Clavien PA: Classification of surgical complications: A new proposal with evaluation in a cohort of 6336 patients and results of a survey. Ann Surg 2004;240:205–213.
21. Goldberg SN, Grassi CJ, Cardella JF, et al.: Image-guided tumor ablation: Standardization of terminology and reporting criteria. Radiology 2005;235:728–739.
22. Liver Cancer Study Group of Japan: General Rules for the Clinical and Pathological study of Primary Liver Cancer, 2nd English edition. Tokyo: Kenehara; 2003.
23. Kitamoto M, Imagawa M, Yamada H, et al.: Radiofrequency ablation in the treatment of small hepatocellular carcinoma: Comparison of the radiofrequency effect with and without chemoembolization. AJR Am J Roentgenol 2003;181:997–1003.
24. Cheng BQ, Jia CQ, Liu CT, et al.: Chemoembolization combined with radiofrequency ablation for patients with hepatocellular carcinoma larger than 3 cm: A randomized controlled trial. JAMA 2008;299:1669–1677.

25. Kojiro M: Focus on dysplastic nodules and early hepatocellular carcinoma: An eastern point of view. Liver Transpl 2004;10: S3–S8.
26. Takayama T, Makuuchi M, Hirohashi SK, et al.: Early hepatocellular carcinoma as an entity with a high rate of surgical cure. Hepatology 1998;28:1241–1246.
27. Wakai T, Shirai Y, Suda T, et al.: Long-term outcomes of hepatectomy vs percutaneous ablation for treatment of hepatocellular carcinoma ≤4 cm. World J Gastroenterol 2006;12:546–552.
28. Shi M, Zhang CQ, Zhang YQ, et al.: Micrometastases of solitary hepatocellular carcinoma and appropriate resection margin. World J Surg 2004;28:376–381.
29. Makuuchi M, Hasegawa H, Yamazaki S: Ultrasonically guided subsegmentectomy. Surg Gynecol Obstet 1985;161:346–350.
30. Makuuchi M, Hasegawa H, Yamazaki S, et al.: The use of operative ultrasound as an aid to liver resection in patients with hepatocellular carcinoma. World J Surg 1987;11:615–621.

Hindawi Publishing Corporation
Journal of Transplantation
Volume 2011, Article ID 483728, 6 pages
doi:10.1155/2011/483728

*Research Article*

# Evidence for the Immunosuppressive Potential of Calcineurin Inhibitor-Sparing Regimens in Liver Transplant Recipients with Impaired Renal Function

**Kentaro Ide, Yuka Tanaka, Takashi Onoe, Masataka Banshodani, Hirofumi Tazawa, Yuka Igarashi, Nabin Bahadur Basnet, Marlen Doskali, Hirotaka Tashiro, and Hideki Ohdan**

*Division of Frontier Medical Science, Department of Surgery, Programs for Biomedical Research, Graduate School of Biomedical Sciences, Hiroshima University, 1-2-3 Kasumi Minami-ku, Hiroshima 734-8551, Japan*

Correspondence should be addressed to Hideki Ohdan, hohdan@hiroshima-u.ac.jp

Received 14 March 2011; Accepted 9 May 2011

Academic Editor: P. Burra



Patients requiring liver transplantation (LT) frequently experience renal insufficiency (RI), which affects their survival. Although calcineurin inhibitor-sparing immunosuppressive regimens (CSRs) are well known to prevent RI, the immune state in recipients receiving CSR remains to be intensively investigated. Among 60 cases of living-donor LT at our institute, 68% of the patients had none to mild RI (non-RI group) and 32% of the patients had moderate to severe RI (RI group). The RI group received a CSR comprising reduced dose of tacrolimus, methylprednisolone, and mycophenolate mofetil, while the non-RI group received a regimen comprising conventional dose of tacrolimus and methylprednisolone. One year after LT, the mean estimated glomerular filtration rate (eGFR) in the RI group had significantly improved, although it was still lower than that of the non-RI group. Serial mixed lymphocyte reaction assays revealed that antidonor T-cell responses were adequately suppressed in both groups. Thus, we provide evidence that CSR leads to improvement of eGFR after LT in patients with RI, while maintaining an appropriate immunosuppressive state.

## 1. Introduction

Renal insufficiency (RI) has been widely recognized as a serious complication of liver transplantation that significantly compromises patient outcome [1–4]. Since a number of patients already have varying degrees of RI, including hepatorenal syndrome, before undergoing liver transplantation, and since postoperative standard immunosuppression protocols based on calcineurin inhibitors (CNIs) can lead to severe tubular atrophy, interstitial fibrosis, and focal hyalinosis of the small renal arteries and arterioles, a majority of liver recipients develop some degree of RI [5–7]. An analysis of data from the Scientific Registry of Transplant Recipients indicates that the cumulative incidence of stage 4 [estimated glomerular filtration rate (eGFR) < 30 mL/min/1.73 $m^2$] or stage 5 chronic kidney disease (eGFR < 15 mL/min/1.73 $m^2$ or need for renal replacement therapy) after liver transplantation is 18% at 5 years [8].

Late renal failure is associated with both pre- and posttransplant factors, including higher concentrations of CNIs both early and late posttransplant and can be predicted by creatinine levels in the first year posttransplant [9, 10]. The recognition of these effects induced interest in strategies using a CNI-sparing immunosuppressive regimen (CSR). Current strategies to overcome CNI toxicity include reduction or withdrawal of CNIs concurrent with switching over to less nephrotoxic drugs like the mammalian target of rapamycin (mTOR) inhibitor or mycophenolate mofetil (MMF) [11–17]. Although these strategies have clearly demonstrated the ability to reduce the incidence of nephrotoxicity in various studies, CSR may result in an increased risk for acute rejection episodes in a subset of patients.

In the present study, we investigated the immune state in liver transplant patients suffering from RI who received a CSR comprising a reduced dose of CNI, methylprednisolone, and MMF. For monitoring the immune-state response to

antidonor allostimulation in these patients, we employed a mixed lymphocyte reaction (MLR) assay using an intracellular carboxyfluorescein diacetate succinimidyl ester (CFSE)-labeling technique. By applying the CFSE-based method, the proliferation of viable $CD4^+$ and $CD8^+$ responder T-cells in response to allostimulation could be separately quantified using multiparameter flow cytometry [18]. The technique allowed us to find that antidonor T-cell responses were adequately suppressed in patients with RI who received the CSR and in patients without RI who received a conventional immunosuppressive regimen.

## 2. Patients and Methods

*2.1. Patients.* Between January 2003 and December 2009, 122 patients underwent living-donor LTs at Hiroshima University Hospital. Of these, 50 patients infected with hepatitis C virus (HCV) and 12 patients who received liver allografts from ABO-blood group incompatible donors were excluded from the study, because they were treated with the diverse immunosuppressive protocols. For the remaining 60 patients, the relationship between RI prior to LT and the clinical/immunological state after LT was investigated. The following information was collected at the time of the transplant: age, sex, etiology of liver disease, model for end-stage liver disease (MELD) score, and diagnosis of hepatocellular carcinoma (HCC) prior to LT. Renal function was evaluated in each participant by determining eGFR. The eGFR of each participant was calculated from their serum creatinine value (SCr) and their age by using the new Japanese equation [19] as follows:

$$\begin{aligned} &\text{eGFR } (\text{mL/min}/1.73\,\text{m}^2) \\ &\quad = 194 \times \text{Age} - 0.287 \\ &\qquad \times \text{S} - \text{Cr} - 1.094 \ (\text{if female} \times 0.739). \end{aligned} \tag{1}$$

In this study, RI was defined as none to mild (eGFR $\geq$ 60 mL/min/1.73 $m^2$) and moderate (30–59 mL/min/1.73 $m^2$) to severe (< 30 mL/min/1.73 $m^2$). The MELD score was calculated for each patient using the United Network for Organ Sharing (UNOS) formula based on the laboratory values obtained just prior to LT. Patients were monitored for renal function using serum creatinine level and eGFR at 1, 3, 6, and 12 months after LT.

*2.2. Immunosuppressive Protocol.* The basic immunosuppressive regimen after LT for the non-RI group comprised tacrolimus (TAC) and methylprednisolone, with gradual tapering of doses. Patients with RI received a CSR comprising a reduced dose of TAC, methylprednisolone, and MMF (Figure 1). In the conventional regimen, the trough whole blood levels of TAC were maintained between 8 and 15 ng/mL in the first few postoperative weeks and between 5 and 10 ng/mL thereafter. In the CSR, the trough whole blood levels of TAC were maintained between 5 and 10 ng/mL in the first few postoperative weeks and between 3 and 5 ng/mL thereafter.

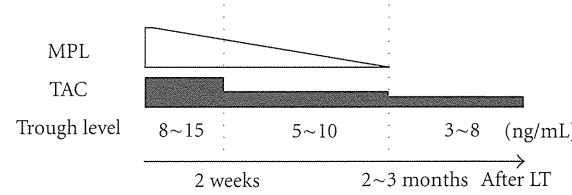


(a) Conventional regimen

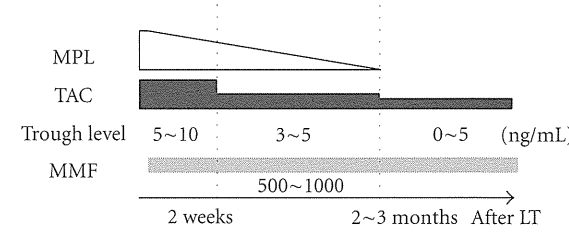


(b) CNI-sparing immunosuppressive regimen

FIGURE 1: Immunosuppressive protocol after liver transplantation. The basic immunosuppressive regimen comprised tacrolimus (TAC) and methylprednisolone (MPL), with doses gradually being tapered off. The trough whole blood levels of TAC were maintained between 8 and 15 ng/mL in the first few postoperative weeks and between 5 and 10 ng/mL thereafter (a). Renal insufficiency (RI) group received CNI-sparing immunosuppressive regimen (CSR) consisting of TAC reduction and concomitant use of mycophenolat mofetil (MMF) (b).

*2.3. Immune Monitoring by an In Vitro MLR Assay.* For monitoring the immune state, an in vitro MLR assay was performed at 1, 3, 6, and 12 months after LT. Briefly, peripheral blood mononuclear cells prepared from the blood of the recipients, donors, and healthy volunteers with the same blood type as the donors (third-party control) for use as the stimulator cells were irradiated with 30 Gy, and those obtained from the recipients for use as responder cells were labeled with 5 lm CFSE (Molecular Probes Inc., Eugene, OR, USA), as described previously [18]. The stimulator and responder cells were incubated for 5 days. CFSE stably stains intracellular proteins without causing toxicity, and the fluorescence intensity of each stained cell segregates equally among daughter cells during cell division, resulting in sequential halving of the cellular fluorescence intensity with every successive generation. After culturing for MLR, the harvested cells were stained with either phycoerythrin- (PE-) conjugated antihuman CD4 or PE-conjugated antihuman CD8 monoclonal antibodies and subjected to analysis by flow cytometry. All analyses were performed on a FACSCalibur flow cytometer (Becton Dickinson, Mountain View, CA, USA). T-cell proliferation was visualized by the serial-halving of the fluorescence intensity of CFSE. $CD4^+$ and $CD8^+$ T-cell proliferation and stimulation index were quantified using a method described previously [18].

*2.4. Statistical Analysis.* Quantitative variables were expressed as mean ± standard deviation (SD) or median (range). Categorical variables were presented as values and

Table 1: Patient characteristics at living donor liver transplantation.

| (eGFR (mL/min/1.73 m$^2$)) | Non-RI group ($n$ = 41) (94.8 ± 26.9) | RI group ($n$ = 19) (42.5 ± 15.9) | $P$ value |
|---|---|---|---|
| Age at LT (years) | 49.2 ± 11.5 | 52.9 ± 9.0 | 0.23 |
| Male sex—$n$ (%) | 21 (51.2) | 13 (68.4) | 0.21 |
| Primary diagnosis—$n$ (%) | | | 0.63 |
| HBV | 15 (36.6) | 9 (47.4) | |
| Alcoholic | 8 (19.5) | 5 (26.3) | |
| AIH | 4 (9.8) | 1 (5.3) | |
| Others | 14 (34.1) | 4 (21.1) | |
| MELD | 16.5 ± 7.1 | 24.7 ± 10.7 | < 0.01 |
| eGFR at 1st year after LT (mL/min/1.73 m$^2$) | 77.2 ± 28.2 | 60.1 ± 13.5 | < 0.01 |
| eGFR > 60 at 1st year after LT—$n$ (%) | 26 (72.2) | 10 (58.8) | 0.33 |
| AR within 1st year—$n$ (%) | 10 (24.4) | 5 (26.3) | 0.87 |
| Bacterial infections—$n$ (%) | 13 (31.7) | 8 (42.1) | 0.43 |
| Fungal infections—$n$ (%) | 4 (9.8) | 4 (21.1) | 0.23 |
| CMV infections—$n$ (%) | 10 (24.4) | 7 (36.8) | 0.32 |

RI, renal insufficiency; LT, liver transplantation; HBV, hepatitis B virus; AIH, Autoimmune hepatitis; eGFR, estimated glomerular filtration rate; MELD, model for end-stage liver disease; AR, acute rejection; CMV, cytomegalovirus. Data are expressed as means ± standard deviation. Difference with $P < 0.05$ was considered significant.

percentages. Student's $t$-test, Mann-Whitney test, chi-square test, and Fischer's exact test were used to compare variables between the two groups. Paired $t$-tests were performed to compare continuous variables throughout the study period. The Kaplan-Meier analyses were used to compare time-to-event variables. $P$ Values < 0.05 were considered statistically significant.

## 3. Results

The 60 patients included 34 males and 26 females; their ages ranged from 20 to 69 (median 52) years. The primary diseases in these patients included hepatitis B virus-related cirrhosis in 24 patients (of these, 18 patients had HCC), alcoholic cirrhosis in 13 patients (of these, 6 patients had HCC), autoimmune hepatitis in 5 patients (of these, 1 patient had HCC), and other diseases in 18 patients.

Before the LTs, 68% of the patients had none to mild RI (non-RI group; mean eGFR, 94.8 ± 26.9 mL/min/1.73 m$^2$) and 32% of the patients had moderate to severe RI (RI group; mean eGFR, 42.5 ± 15.9 mL/min/1.73 m$^2$). The characteristics of these patients are listed in Table 1. There was a difference in MELD score between the groups. Mean TAC trough levels during the first year after LT in the non-RI and RI groups are shown in Figure 2(a). There were differences in mean TAC trough levels during 3 months after LT between the groups. One year after the LDLTs, the mean eGFR in the non-RI group had significantly deteriorated (from 94.8 ± 26.9 to 77.2 ± 28.2 mL/min/1.73 m$^2$, $P < 0.01$). In contrast, the mean eGFR in the RI group had significantly improved after LT (from 42.5 ± 15.9 to 60.1 ± 13.5 mL/min/1.73 m$^2$, $P < 0.01$), although it was still lower than that of the non-RI group (Figure 2(b)). Notably, 53% of the patients in the RI group were completely cured of RI by 1 year after LT. None of the patients had severe RI at 1 year after LT nor required chronic hemodialysis during the observation period.

To evaluate the immune status of these patients, we employed a serial MLR assay using a CFSE-labeling technique. Lack of proliferation of both CD4$^+$ and CD8$^+$ T-cells in the antidonor CFSE-MLR assay indicates suppression of the antidonor response, whereas a remarkable proliferation of these T-cells reflects a strong antidonor response. In both groups, limited CD4$^+$ and CD8$^+$ T-cell proliferation was observed in the antidonor responses as compared with the anti-third-party responses through the first year. At 1 month after LT, the average of stimulation index (SI) for CD4$^+$ T-cells in response to anti-third-party stimulation was >2 (the average value in healthy volunteers without any immunosuppressive treatment) that is, there was a normal response in the anti-third-party (Figures 3(a) and 3(b)). At 1 year after LT, the average of SIs for CD4$^+$ and CD8$^+$ T-cells in response to both antidonor and anti-third-party stimulation was <2 (Figures 3(c) and 3(d)). There were no significant differences in acute rejection rates, bacterial, fungal, or cytomegalovirus infection rates and patient survival between the groups (Table 1).

## 4. Discussion

Chronic RI is a serious complication in liver transplantation that significantly compromises patient survival and outcome. Depending on the criteria applied for a definition of chronic renal insufficiency and the duration of followup, the reported rate of chronic renal insufficiency after liver transplantation may vary from 10% to 80% [1, 20–22]. CNI toxicity has been defined as one of the possible risk factors for renal insufficiency in long-term liver transplant survivors. It has been shown that exposure to CNIs within the first 6 months

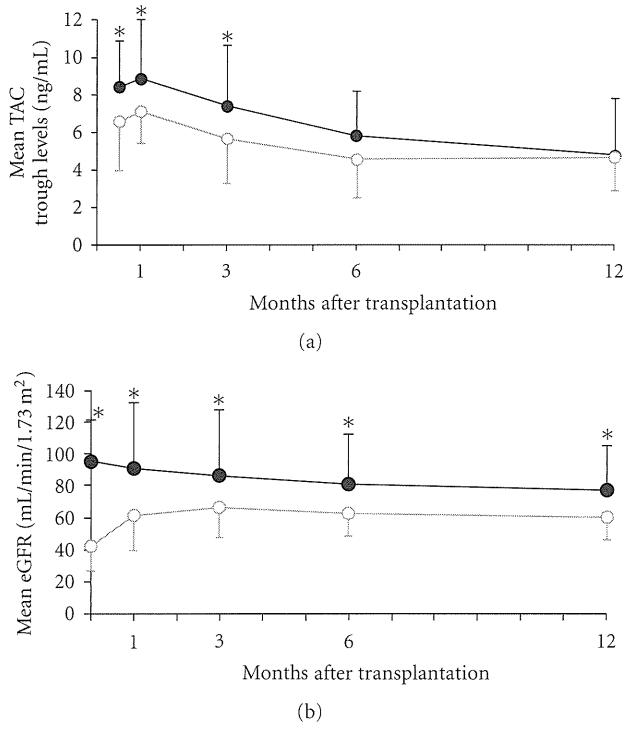


FIGURE 2: Kinetics of mean trough levels of tacrolimus and mean estimated glomerular filtration rate (eGFR) in the RI group and non-RI group during the first year after transplantation. (a) Mean trough levels of tacrolimus in the non-RI group (black line) and RI group (gray line). (b) Mean estimated glomerular filtration rate (eGFR) in the non-RI group (black line) and RI group (gray line). Data are median ± SD of values. $^*P < 0.05$.

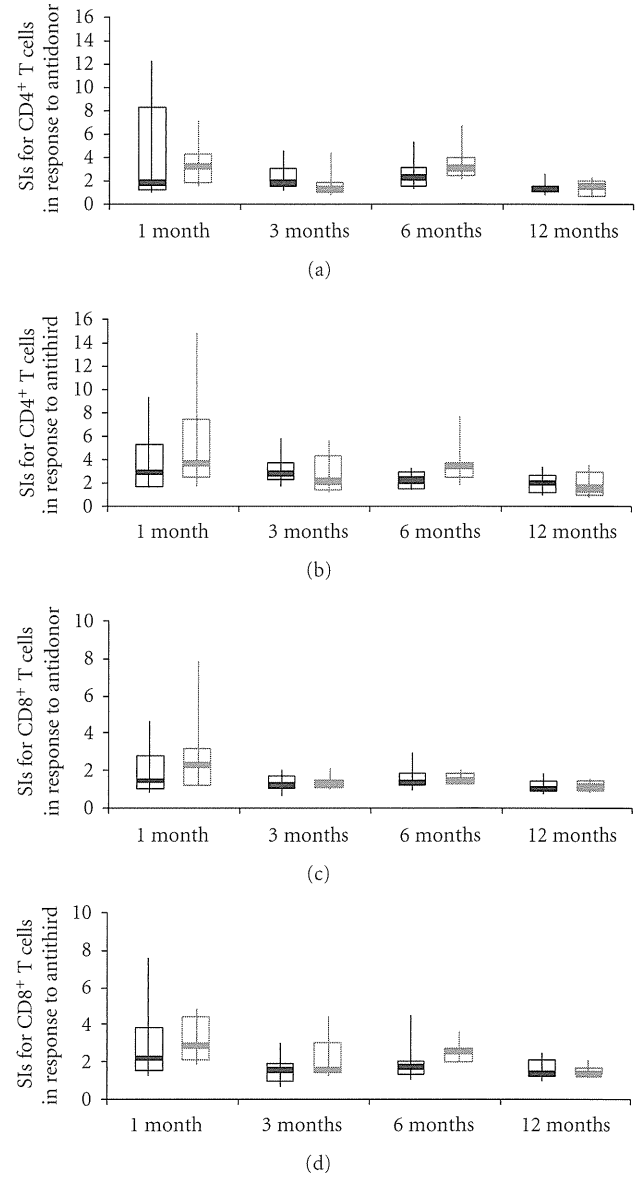


FIGURE 3: Kinetics of stimulation index in the RI group and non-RI group during the first year after transplantation. Stimulation index (SI) of each of the $CD4^+$ T-cell (a, b) and $CD8^+$ T-cell (c, d) subsets in the antidonor (a, c) and anti-third-party (b, d) MLR in patients in non-RI group (black line) and RI group (gray line). $CD4^+$ and $CD8^+$ T-cell proliferation and their SIs were quantified as follows. The number of division precursors was extrapolated from the number of daughter cells of each division, and the number of mitotic events in each of the $CD4^+$ and $CD8^+$ T-cell subsets was calculated. Using these values, the mitotic index was calculated by dividing the total number of mitotic events by the total number of precursors. The SIs of allogeneic combinations were calculated by dividing the mitotic index of a particular allogeneic combination by that of the self-control. The box plot represents the 25th to 75th percentile, the dark line is the median, and the extended bars represent the 10th to the 90th percentile.

after liver transplantation represents a risk factor for renal failure [23]. The GFR at 1 year had a better correlation with later renal function than the pretransplant GFR [24]. The recognition of these facts induced interest in preventing CNI toxicity. It has also reported that the use of adjunctive MMF immediately after LT might protect against CNI nephrotoxicity, potentially without the need for dose reduction or increased risk of adverse events [25]. Therefore, current strategies to overcome CNI toxicity include reduction or withdrawal of CNIs along with switching to mTOR inhibitor or MMF-based regimens [11, 12, 14, 15, 26–28]. These strategies have been documented in several recent and ongoing trials to achieve an improvement in renal function in a large proportion of liver transplant patients.

In our CSR using MMF, wherein our study results agree with the results from previous studies, patients with pre-transplant renal insufficiency were associated with less impairment of renal function without an increased frequency of rejection, infection, or patient survival. In addition to this clinical evidence for the usefulness of the CSR using MMF, the present study provides immunological evidence, by analyzing the data obtained from an MLR assay, that antidonor T-cell responses were adequately suppressed in patients who received the CSR and in patients who received the conventional immunosuppressive regimen. Notably, the individual variations of SIs of $CD4^+$ T-cell and $CD8^+$ T-cell subsets on antidonor T-cell responses in patients who received the CSR were smaller than those in patients who

received the conventional regimen, although the average values of both were similar. This might be explained by the possibility that the CSR comprising triple immunosuppressive drugs was equally effective in a wide variety of patients.

Several limitations of this study are present. Our sample size was relatively small without long-term followup, and single-center retrospective data are reported. Since the 2 groups of patients are not perfectly comparable as renal impairment can reduce immune responses, we could not rule out a possibility that reduced CNI, without necessarily adding MMF, may be sufficient for the treatment of these patients.

We excluded HCV positive cases and ABO-blood group incompatible cases from the study because of diverse protocol (In brief, in patients with HCV infection, methylprednisolone is not administered, which may be beneficial for preventing enhanced viral replication. Instead, basiliximab and MMF are usually administered to such patients. In ABO-blood group incompatible cases, anti-CD20 monoclonal antibody is administered for eliminating temporarily B cells 2 weeks before transplantation, and simultaneously commencing administration of CNI and MMF.). Hence, the effect of CSR in RI patients with those backgrounds remains to be elucidated. Nevertheless, this first evaluation of the immune state in liver transplant patients suffering from RI received a CSR was essential before to propose an evaluation at a larger scale.

In conclusion, patients with pre-transplant RI receiving CSR under immunological monitoring using an MLR assay were associated with less impairment of renal function without an increased frequency of rejection or patient survival. Antidonor T-cell responses were adequately suppressed in these patients as well as in patients who received the conventional immunosuppressive regimen comprising a standard dose of CNI.

## Abbreviations

AIH: Autoimmune hepatitis
AR: acute rejection
CFSE: carboxyfluorescein diacetate succinimidyl ester
CMV: cytomegalovirus
CNI: calcineurin inhibitor
CSR: CNI sparing immunosuppressive regimen
eGFR: estimated glomerular filtration rate
HBV: hepatitis B virus
HCV: hepatitis C virus
LT: liver transplantation
MELD: model for end-stage liver disease
MLR: mixed lymphocyte reaction
MMF: mycophenolate mofetil
mTOR: mammalian target of rapamycin
MPL: methylprednisolone
RI: renal insufficiency
SI: stimulation index
TAC: tacrolimus.

## References

[1] K. P. Platz, A. R. Mueller, G. Blumhardt et al., "Nephrotoxicity following orthotopic liver transplantation: a comparison between cyclosporine and FK506," *Transplantation*, vol. 58, no. 2, pp. 170–178, 1994.

[2] N. C. Fisher, P. G. Nightingale, B. K. Gunson, G. W. Lipkin, and J. M. Neuberger, "Chronic renal failure following liver transplantation: a retrospective analysis," *Transplantation*, vol. 66, no. 1, pp. 59–66, 1998.

[3] T. A. Gonwa, G. B. Klintmalm, M. Levy, L. S. Jennings, R. M. Goldstein, and B. S. Husberg, "Impact of pretransplant renal function on survival after liver transplantation," *Transplantation*, vol. 59, no. 3, pp. 361–365, 1995.

[4] S. Nair, S. Verma, and P. J. Thuluvath, "Pretransplant renal function predicts survival in patients undergoing orthotopic liver transplantation," *Hepatology*, vol. 35, no. 5, pp. 1179–1185, 2002.

[5] B. D. Myers, "Cyclosporine nephrotoxicity," *Kidney International*, vol. 30, pp. 964–974, 1986.

[6] J. B. Puschett, A. Greenberg, J. Holley, and J. McCauley, "The spectrum of ciclosporin nephrotoxicity," *American Journal of Nephrology*, vol. 10, no. 4, pp. 296–309, 1990.

[7] M. K. Porayko, T. A. Gonwa, G. B. Klintmalm, and R. H. Wiesner, "Comparing nephrotoxicity of FK 506 and cyclosporine regimens after liver transplantation: preliminary results from US multicenter trial," *Transplantation Proceedings*, vol. 27, no. 1, pp. 1114–1116, 1995.

[8] A. O. Ojo, P. J. Held, F. K. Port et al., "Chronic renal failure after transplantation of a nonrenal organ," *The New England Journal of Medicine*, vol. 349, no. 10, pp. 931–940, 2003.

[9] T. A. Gonwa, M. L. Mai, L. B. Melton et al., "End-stage renal disease (ESRD) after orthotopic liver transplantation (OLTX) using calcineurin-based immunotherapy: risk of development and treatment," *Transplantation*, vol. 72, no. 12, pp. 1934–1939, 2001.

[10] A. Pawarode, D. M. Fine, and P. J. Thuluvath, "Independent risk factors and natural history of renal dysfunction in liver transplant recipients," *Liver Transplantation*, vol. 9, no. 7, pp. 741–747, 2003.

[11] S. A. Farkas, A. A. Schnitzbauer, G. Kirchner, A. Obed, B. Banas, and H. J. Schlitt, "Calcineurin inhibitor minimization protocols in liver transplantation," *Transplant International*, vol. 22, no. 1, pp. 49–60, 2009.

[12] H. J. Schlitt, A. Barkmann, K. H. W. Böker et al., "Replacement of calcineurin inhibitors with mycophenolate mofetil in liver-transplant patients with renal dysfunction: a randomised controlled study," *The Lancet*, vol. 357, no. 9256, pp. 587–591, 2001.

[13] S. Beckebaum, V. Cicinnati, E. Brokalaki, A. Frilling, G. Gerken, and C. E. Broelsch, "CNI-sparing regimens within the liver transplant setting: experiences of a single center," *Clinical Transplants*, pp. 215–220, 2004.

[14] C. L. Liu, S. T. Fan, C. M. Lo et al., "Interleukin-2 receptor antibody (basiliximab) for immunosuppressive induction therapy after liver transplantation: a protocol with early elimination of steroids and reduction of tacrolimus dosage," *Liver Transplantation*, vol. 10, no. 6, pp. 728–733, 2004.

[15] G. P. Pageaux, L. Rostaing, Y. Calmus et al., "Mycophenolate mofetil in combination with reduction of calcineurin inhibitors for chronic renal dysfunction after liver transplantation," *Liver Transplantation*, vol. 12, no. 12, pp. 1755–1760, 2006.

[16] S. M. Flechner, J. Kobashigawa, and G. Klintmalm, "Calcineurin inhibitor-sparing regimens in solid organ transplantation: focus on improving renal function and nephrotoxicity," *Clinical Transplantation*, vol. 22, no. 1, pp. 1–15, 2008.

[17] S. Karie-Guigues, N. Janus, F. Saliba et al., "Long-term renal function in liver transplant recipients and impact of immunosuppressive regimens (calcineurin inhibitors alone or in combination with mycophenolate mofetil): The TRY study," *Liver Transplantation*, vol. 15, no. 9, pp. 1083–1091, 2009.

[18] Y. Tanaka, H. Ohdan, T. Onoe et al., "Low incidence of acute rejection after living-donor liver transplantation: immunologic analyses by mixed lymphocyte reaction using a carboxyflourescein diacetate succinimidyl ester labeling technique," *Transplantation*, vol. 79, no. 9, pp. 1262–1267, 2005.

[19] S. Matsuo, E. Imai, M. Horio et al., "Revised Equations for Estimated GFR From Serum Creatinine in Japan," *American Journal of Kidney Diseases*, vol. 53, no. 6, pp. 982–992, 2009.

[20] J. McCauley, D. H. Van Thiel, T. E. Starzl, and J. B. Puschett, "Acute and chronic renal failure in liver transplantation," *Nephron*, vol. 55, no. 2, pp. 121–128, 1990.

[21] A. M. De Mattos, A. J. Olyaei, and W. M. Bennett, "Nephrotoxicity of immunosuppressive drugs: long-term consequences and challenges for the future," *American Journal of Kidney Diseases*, vol. 35, no. 2, pp. 333–346, 2000.

[22] A. J. Olyaei, A. M. De Mattos, and W. M. Bennett, "Nephrotoxicity of immunosuppressive drugs: new insight and preventive strategies," *Current Opinion in Critical Care*, vol. 7, no. 6, pp. 384–389, 2001.

[23] A. Wilkinson and P. T. Pham, "Kidney dysfunction in the recipients of liver transplants," *Liver Transplantation*, vol. 11, no. 11, pp. S47–S51, 2005.

[24] F. Åberg, A. M. Koivusalo, K. Höckerstedt, and H. Isoniemi, "Renal dysfunction in liver transplant patients: comparing patients transplanted for liver tumor or acute or chronic disease," *Transplant International*, vol. 20, no. 7, pp. 591–599, 2007.

[25] S. Haywood, M. Abecassis, and J. Levitsky, "The renal benefit of mycophenolate mofetil after liver transplantation," *Clinical Transplantation*, vol. 25, no. 1, pp. E88–E95, 2011.

[26] V. Schmitz, S. Laudi, F. Moeckel et al., "Chronic renal dysfunction following liver transplantation," *Clinical Transplantation*, vol. 22, no. 3, pp. 333–340, 2008.

[27] G. Orlando, L. Baiocchi, A. Cardillo et al., "Switch to 1.5 grams MMF monotherapy for CNI-related toxicity in liver transplantation is safe and improves renal function, dyslipidemia, and hypertension," *Liver Transplantation*, vol. 13, no. 1, pp. 46–54, 2007.

[28] G. S. Jensen, A. Wiseman, and J. F. Trotter, "Sirolimus conversion for renal preservation in liver transplantation: not so fast," *Liver Transplantation*, vol. 14, no. 5, pp. 601–603, 2008.

Research Article

EASL EUROPEAN ASSOCIATION FOR THE STUDY OF THE LIVER | JOURNAL OF HEPATOLOGY

# Rho inhibitor prevents ischemia–reperfusion injury in rat steatotic liver

Shintaro Kuroda, Hirotaka Tashiro*, Yuka Igarashi, Yoshisato Tanimoto, Junko Nambu, Akihiko Oshita, Tsuyoshi Kobayashi, Hironobu Amano, Yuka Tanaka, Hideki Ohdan

*Department of Surgery, Division of Frontier Medical Science, Programs for Biomedical Research, Graduate School of Biomedical Sciences, Hiroshima University, Hiroshima, Japan*

**Background & Aims**: Hepatic stellate cells are thought to play a role in modulating intrahepatic vascular resistance based on their capacity to contract via Rho signaling. We investigated the effect of a Rho-kinase inhibitor on ischemia–reperfusion injury in the steatotic liver.

**Methods**: Steatotic livers, induced by a choline-deficient diet in rats, were subjected to ischemia–reperfusion injury. Hepatic stellate cells isolated from steatotic livers were analyzed for contractility and Rho signaling activity. The portal pressure of the perfused rat liver and the survival rate after ischemia–reperfusion were also investigated.

**Results**: Hepatic stellate cells from steatotic livers showed increased contractility and upregulation of Rho-kinase 2 compared with those from normal livers. Furthermore, endothelin-1 significantly enhanced the contractility and phosphorylation level of myosin light chain and cofilin in hepatic stellate cells isolated from steatotic livers. A specific Rho-kinase inhibitor, fasudil, significantly suppressed the contractility and decreased the phosphorylation levels of myosin light chain and cofilin. Serum levels of endothelin-1 were markedly increased after IR in rats with steatotic livers, whereas fasudil significantly decreased endothelin-1 serum levels. Rats with steatotic livers showed a significant increase in portal perfusion pressure after ischemia–reperfusion and a significant decrease in survival rate; fasudil treatment significantly reduced these effects.

**Conclusions**: Activation of Rho/Rho-kinase signaling in hepatic stellate cells isolated from steatotic livers is associated with an increased susceptibility to ischemia–reperfusion injury. A Rho-kinase inhibitor attenuated the activation of hepatic stellate cells isolated from steatotic livers and improved ischemia–reperfusion injury in steatotic rats.





## Introduction

Liver steatosis increases the risk of postoperative morbidity and mortality after liver surgery including liver transplantation [1–3]. Ischemia–reperfusion (IR) injury is one of the most critical complications commonly associated with liver surgery [4–6]. Although it is known that steatotic liver (SL) is particularly vulnerable to IR injury, the mechanisms underlying this increased susceptibility have not yet been clarified.

Experimental studies have indicated that the degree of steatosis is correlated with hepatic microcirculatory disturbances [4,5]. Fat droplet accumulation in the cytoplasm of hepatocytes is associated with an increase in cell volume, which may result in the partial or complete obstruction of the hepatic sinusoidal space and the reduction of sinusoidal blood flow. A continuous state of chronic cellular hypoxia persists in fatty hepatocytes, predisposing the SL to IR injury [7]. The sinusoidal lumens are narrowed by fibrin microthrombi and cellular debris during reperfusion, further decreasing sinusoidal perfusion.

Hepatic stellate cells (HSCs) play an important role in the regulation of hepatic microcirculation. HSCs undergo contraction or relaxation in response to certain stimuli and, as a result, regulate microcirculation by increasing or decreasing the diameter of the sinusoidal lumen [8]. HSCs also play an important role in IR injury [9]. Because HSCs are oxygen-sensing cells [10], they are likely to be activated by exposure to IR-induced oxidative stress, resulting in the disruption of hepatic microcirculation.

The Rho family of small GTPases is known to regulate cell shape and motility through reorganization of the actin cytoskeleton [11]. One of the putative Rho target proteins, the serine/threonine kinase ROCK, mediates cytoskeleton-dependent cell functions by enhancing the phosphorylation of myosin light

Keywords: Steatosis; Ischemia–reperfusion injury; Hepatic stellate cell; Rho-kinase; Fasudil.

*Received 19 November 2010; received in revised form 7 April 2011; accepted 29 April 2011; available online 12 July 2011*

* Corresponding author. Address: Department of Surgery, Division of Frontier Medical Science, Programs for Biomedical Research, Graduate School of Biomedical Sciences, Hiroshima University, 1-2-3 Kasumi, Hiroshima 734-8551, Japan. Tel.: +81 82 257 5222; fax: +81 82 257 5224.

*E-mail address:* htashiro@hiroshima-u.ac.jp (H. Tashiro).

*Abbreviations:* IR, ischemia–reperfusion; SL, steatotic liver; HSCs, hepatic stellate cells; ROCK, Rho-kinase; MLC, myosin light chain; P-MLC, phosphorylated myosin light chain; NL, normal liver; fasudil, fasudil hydrochloride hydrate; NO, nitric oxide; L-NAME, *N*-nitro-L-arginine methyl ester; ET-1, endothelin-1; P-Cofilin, phosphorylated cofilin; AST, aspartate aminotransferase; ALT, alanine aminotransferase; H&E, hematoxylin and eosin; TUNEL, TdT-mediated dUTP-digoxigenin nick-end labeling; HSCs-SL, hepatic stellate cells isolated from rat steatotic liver; HSCs-NL, hepatic stellate cells isolated from rat normal liver; SECs, sinusoidal endothelial cells.

ELSEVIER

Journal of Hepatology **2012** vol. 56 | 146–152

chain (MLC) [12]. An increase in phosphorylated MLC (P-MLC) increases the contractility of actomyosin and causes smooth muscle contraction [13]. In addition, P-MLC facilitates the clustering of integrins and the bundling of actin fibers [14], resulting in stimulus-induced cell adhesion and motility.

The contraction of HSCs narrows the sinusoidal lumen and reduces hepatic microcirculatory flow via Rho signaling. We reported previously that the Rho/ROCK signaling pathway played an important role in the activation of HSCs and that a ROCK inhibitor attenuated hepatic injury after warm IR and orthotopic liver transplantation in a rat model [9]. Recently, HSC activation has been shown to be correlated with the severity of steatosis in the liver [15–17]. However, little is known about the connection between activated HSCs and IR injury in SL. Furthermore, there are few studies on the involvement of Rho signaling in the activation of HSCs in SL.

The aim of the present study was to investigate the association between Rho signaling and the activation of HSCs in SL. We also examined whether inhibition of the Rho/ROCK pathway could ameliorate IR injury in the steatotic rat liver.

## Materials and methods

*Animals*

Four-week-old male Wistar rats were purchased from Charles River Breeding Laboratories (Osaka, Japan). Rats were fed either a choline-deficient diet (Hiroshima Institute for Experimental Animals, Hiroshima, Japan) to encourage the development of SL, or a normal diet, which resulted in the development of a normal liver (NL). All animal experiments were performed according to the guidelines set by the US National Institutes of Health (1996).

*Liver IR*

Under anesthesia, whole rat livers were subjected to warm ischemia by clamping the hepatic artery and portal vein with microvascular clips. The specific ROCK inhibitor fasudil hydrochloride hydrate (fasudil; kindly donated by Asahi Kasei Co., Tokyo, Japan) was used to investigate the effect of ROCK inhibition on liver IR injury. Selected rats were pretreated with 10 mg/kg fasudil (intraperitoneal injection) 30 min before the induction of ischemia.

*Isolation of HSCs*

HSCs were isolated from rat livers according to previously described procedures [9,18]. Purity was estimated by ordinal light and fluorescence microscopic examination and by indirect enzyme immunoreactivity with an antidesmin antibody (Dako, Versailles, France). HSCs were grown in standard tissue culture plastic flasks in Dulbecco's minimum essential medium with 10% fetal bovine serum and antibiotics.

*Collagen gel contraction assay*

The contractility of the HSCs was evaluated using hydrated collagen gel lattices on 24-well culture plates as described previously with some modifications [9,19]. To investigate the influence of nitric oxide (NO) on HSCs, the NO synthase inhibitor *N*-nitro-L-arginine methyl ester (L-NAME; Cayman Chemical, Ann Arbor, MI) was used.

*Western blot analysis*

Primary rat HSCs were left untreated or were treated with 10 μM fasudil and/or 5 nM endothelin-1 (ET-1; Sigma–Aldrich Inc., Tokyo, Japan) for 30 min before homogenization in lysis buffer (Cell Lysis Buffer; Cell Signaling Technology, Danvers, MA). Western blot analysis was performed according to previously described procedures with some modifications [20]. Specific antibodies against β-actin were from Abcam (Tokyo, Japan); those against MLC were from Sigma–Aldrich Inc., and those against P-MLC, cofilin, phosphorylated cofilin (P-Cofilin), and Rho-kinase 2(ROCK2) were from Cell Signaling Technology. The protein expression of ROCK2 was normalized to the level of β-actin. The phosphorylation levels were normalized to the levels of total MLC or cofilin protein expression.

*Biochemical assessment*

Blood samples were collected from the inferior vena cava. Serum ET-1 concentrations were measured using an Endothelin-1 EIA kit (Phoenix Pharmaceuticals, Inc., Burlingame, CA) according to the manufacturer's instructions. Aspartate aminotransferase (AST) and alanine aminotransferase (ALT) levels were assayed by standard enzymatic methods.

*Measurement of portal perfusion pressure in the isolated rat liver*

Portal pressure in isolated perfused rat livers was measured according to previously described procedures, with some modifications [21]. The perfusion with Krebs–Henseleit buffer (Sigma–Aldrich Inc.) was continued until the monitored inlet pressure value became stable at a constant flow rate of 0.3 ml $min^{-1}$ liver $volume^{-1}$ (ml).

*Confocal immunofluorescence and histological study*

Phalloidin staining of isolated HSCs and liver sections was performed according to previously described procedures [22]. Samples were observed under a conventional fluorescence microscope or a laser confocal microscope. For the histological study, liver specimens were collected from the middle hepatic lobe after IR. Formalin-fixed liver tissue sections were stained with hematoxylin and eosin (H&E) and examined microscopically. To assess the activity of HSCs in liver sections, phalloidin staining was performed. To assess the grade of the steatosis, sections were stained for oil red O. Furthermore, the detection of apoptosis in liver tissue sections was achieved by TdT-mediated dUTP-digoxigenin nick-end labeling (TUNEL) staining as previously reported [23].

*Statistical analysis*

Survival rates were compared using the Kaplan–Meier method and analyzed by the log-rank test. Other data are expressed as average values (SD). Statistical analysis among experimental groups was performed using the *t*-test. *p* values less than 0.05 were considered statistically significant. Statistical analyses were performed using SPSS software, version 16 (SPSS Japan Inc., Tokyo, Japan).

## Results

*Changes in the morphology of HSCs isolated from steatotic rat livers*

At 10 weeks, rats fed a choline-deficient diet developed liver steatosis, characterized by more than 60% of fatty filtration in the hepatocytes with few inflammatory cells and slight fibrosis (Fig. 1A). HSCs isolated from rat SLs (HSCs-SL) showed increased stress fiber formation and F-actin expression compared to HSCs isolated from normal rat livers (HSCs-NL), which were suppressed by fasudil treatment (Fig. 1B). Phalloidin staining of liver sections showed stress fiber formation and F-actin expression around sinusoidal spaces in SL after IR, as well as the suppression of these changes by fasudil (Supplementary Fig. 1).

*Contractility of HSCs isolated from normal and steatotic rat livers*

To evaluate differences in contractility, HSCs-NL and HSCs-SL were cultured on hydrated collagen gels. Contraction was measured as the reduction in the initial area of the gel. In the absence of vasoactive agents, the areas of the gels with HSCs-SL were

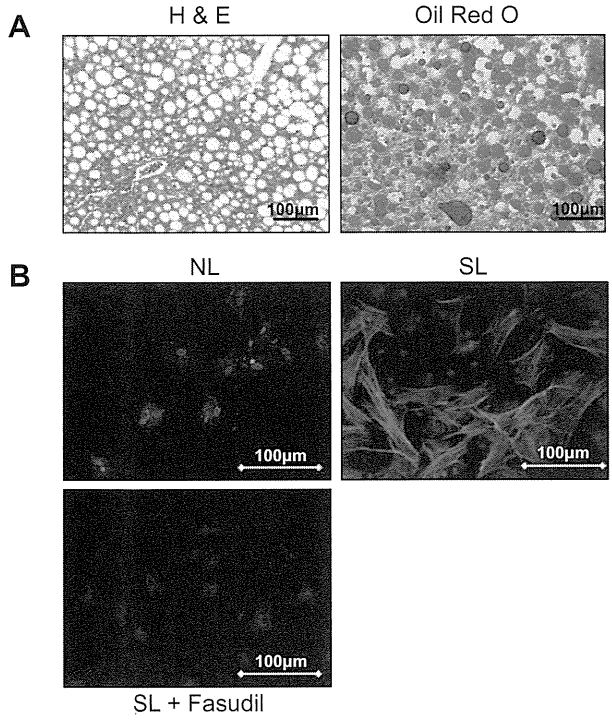


**Fig. 1. Oil red O staining and morphology changes of HSCs isolated from rat SL.** (A) Representative H&E- and oil red O-stained sections. Rats fed a choline-deficient diet for 6 weeks had more than 60% of macrovesicular steatosis. (B) Images show differences in F-actin expression in isolated HSCs from NL, SL, and SL treated with fasudil (10 μM, 24 h). Cells were stained to show F-actin (red) and nuclei (blue). HSCs isolated from NL showed slight stress fiber formation and F-actin expression. By contrast, HSCs isolated from SL had an elongated, fusiform morphology with prominent dendritic processes. Fasudil suppressed both stress fiber formation and F-actin expression. (For interpretation of the references to colour in this figure legend, the reader is referred to the web version of this article.)

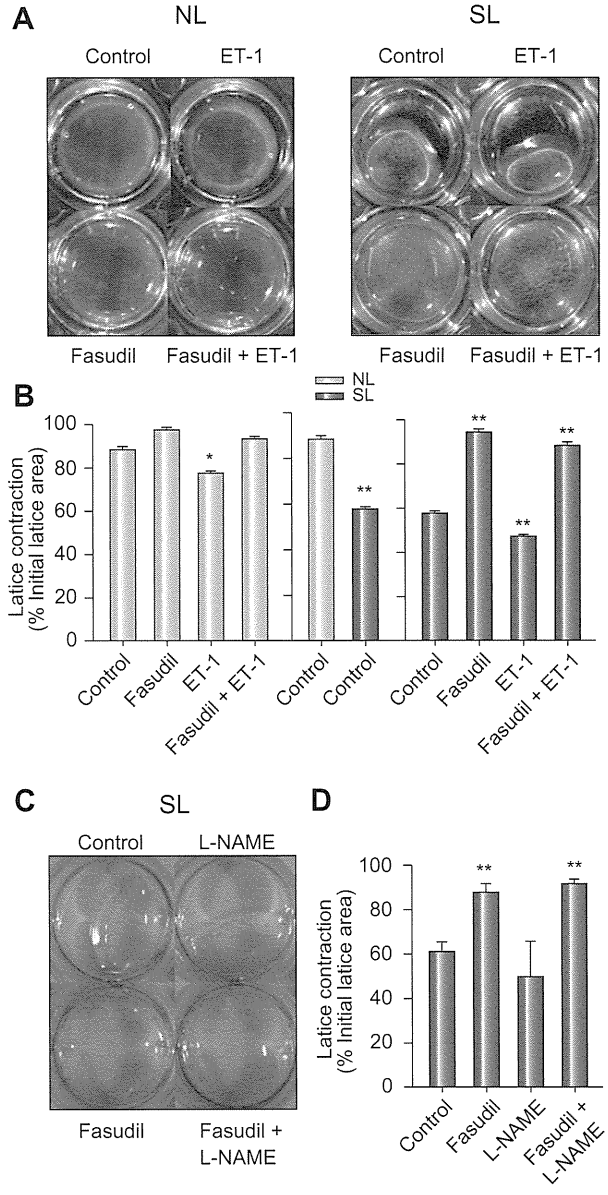


**Fig. 2. Collagen gel contraction assay.** (A) Contraction of collagen gels induced by the activation of isolated HSCs in untreated NL and SL, and in NL and SL treated with ET-1, fasudil or a combination of the two. Without the addition of HSCs, the collagen gels did not contract during the observation period (not shown). Control, medium alone; ET-1, 5 nM ET-1; Fasudil, 10 μM fasudil; Fasudil + ET-1, 10 μM fasudil and 5 nM ET-1. (C) Contraction of collagen gels in SL and SL treated with L-NAME, fasudil or a combination of the two. Control, medium alone; L-NAME, 100 μM L-NAME; Fasudil, 10 μM fasudil; Fasudil + L-NAME, 10 μM fasudil, and 100 μM L-NAME. (B and D) Changes in the collagen gel area induced by contraction of HSCs. HSCs isolated from rat NL, closed bars; HSCs isolated from rat SL, open bars. Average values (SD) of three independent experiments are shown. $^{*}p$ <0.05 compared to each control; $^{**}p$ <0.01 compared to each control.

significantly smaller than those with HSCs-NL ($p$ <0.01). In the presence of fasudil (10 μM), this reduction in the areas of gels with HSCs-SL was not observed. The gel areas containing HSCs-SL were significantly smaller in the presence of ET-1 (5 nM) than those with HSCs-SL in the absence of ET-1 ($p$ <0.01). In sharp contrast, however, when fasudil was added to the culture medium in the presence of ET-1, the shrinkage of the gels with HSCs-SL was suppressed ($p$ <0.01; Fig. 2A and B). Furthermore, the NO synthase inhibitor L-NAME (100 μM) was used to investigate the influence of NO on HSCs. Fasudil suppressed the contraction of HSCs-SL even in the presence of L-NAME ($p$ <0.01; Fig. 2C and D).

*Expression of ROCK2 and phosphorylation of MLC and cofilin*

To examine the possible involvement of the Rho/ROCK pathway in the activation of HSCs, the expression of ROCK2 and the phosphorylation state of MLC and cofilin, a downstream effector of Rho/ROCK signaling, were assessed by Western blot analysis with monoclonal antibodies to ROCK2 and the phosphorylated form of MLC and cofilin. Quantitative analysis using a scanning densitometer confirmed that ROCK2 was significantly overexpressed in HSCs-SL compared with HSCs-NL ($p$ <0.01) (Fig. 3A). The phosphorylation level of MLC in HSCs-SL was significantly increased compared with that in HSCs-NL. The phosphorylation levels of MLC and cofilin were significantly enhanced by ET-1 in HSCs-SL

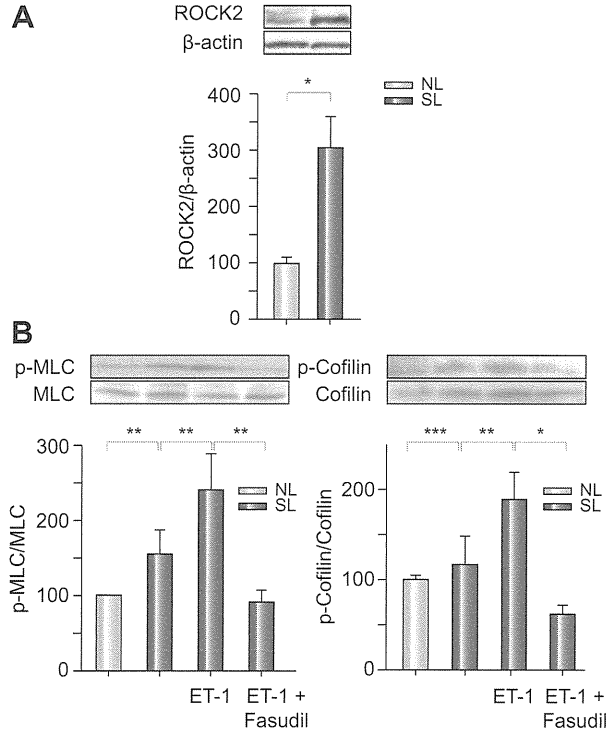


**Fig. 3. Western blot analyses in rat HSCs isolated from rat NL or SL.** (A) Expression level of ROCK2. (B) Total and phosphorylated MLC and cofilin. HSCs isolated from rat SL were either left untreated or cultured with 10 μM fasudil and/or 5 nM ET-1 for 30 min. The protein expression of ROCK2 was normalized to the level of β-actin. The phosphorylation levels of MLC and cofilin were normalized to total MLC and cofilin protein expression, respectively. Each figure is representative of three independent experiments. Average values (SD) for individual groups are shown. *$p$ <0.01, **$p$ <0.05, ***N.S.

($p$ <0.05, in both), but the effects were suppressed by fasudil ($p$ <0.05, 0.01, respectively; Fig. 3B).

*Influence of IR on the secretion of ET-1*

Serum ET-1 concentrations were measured after 30 min of ischemia followed by 3 h of reperfusion using ELISA. Serum ET-1 concentrations significantly increased after IR in rats with NL ($p$ <0.01). Serum ET-1 concentrations after IR were significantly higher in rats with SL than in rats with NL ($p$ <0.01). Furthermore, fasudil significantly suppressed the serum ET-1 concentrations after IR ($p$ <0.01; Fig. 4).

*Influence of IR on portal perfusion pressure*

To determine the influence of IR on the microvascular blood flow in the hepatic lobule, the portal perfusion pressure was assessed in isolated rat livers. Perfusion pressures were measured after 45 min of ischemia followed by 15 min of reperfusion. The portal perfusion pressures in rats with SL were significantly higher than those in rats with NL ($p$ <0.05). The portal perfusion pressures in rats with SL after IR were significantly higher than those in rats with SL that did not undergo IR ($p$ <0.01), and the effect was suppressed by fasudil ($p$ <0.01; Fig. 5).

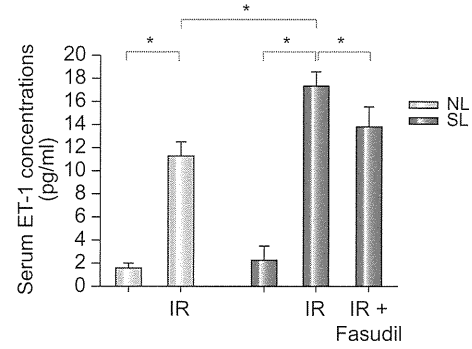


**Fig. 4. Serum ET-1 concentrations, reflecting secretion from SECs and HSCs.** Blood samples were collected from rats with NL or SL after 30 min of ischemia followed by 3 h of reperfusion. A group of the SL rats received fasudil (10 mg/kg) 30 min before ischemia. Average values (SD) for individual groups are shown; for all groups, n = 6. *$p$ <0.01.

*Biochemical assessment, histological study, and survival rates after IR*

AST and ALT are well-established markers of hepatocellular injury after IR. Serum AST and ALT levels were measured after 30 min of ischemia followed by 3 or 24 h of reperfusion. The increase in AST at 3 and 24 h and in ALT at 3 h after IR of the untreated rats with SL was significantly higher than in fasudil-treated rats with SL (Fig. 6A). For histological analysis, liver specimens were obtained after 45 min of ischemia followed by 24 h of reperfusion. Liver specimens from untreated rats with SL after IR showed distortion of architecture, sinusoidal congestion, microthrombus, and extensive areas of coagulative necrosis. In contrast, specimens from the SL group treated with 10 mg/kg fasudil showed almost normal hepatic structure (Fig. 6B). TUNEL staining of liver tissue sections after IR showed that most hepatocytes in NL were TUNEL positive, whereas only minimal TUNEL staining was found in SL (Supplementary Fig. 2). The survival rate of rats with SL that underwent 45 min of ischemia was significantly lower than that of rats with NL ($p$ <0.01). However, treat-

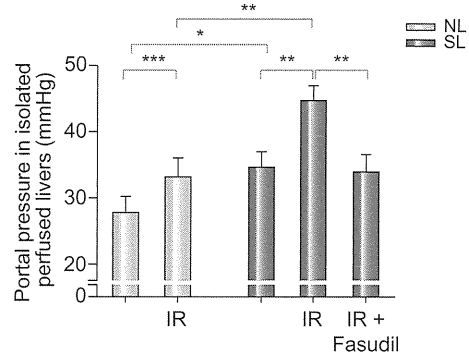


**Fig. 5. Portal pressures in isolated perfused livers from rats with NL and SL.** Livers were untreated, treated with 45 min of ischemia followed by 15 min of reperfusion, or preinjected with 10 mg/kg fasudil intraperitoneally 30 min before IR. Average values (SD) for individual groups are shown; for all groups, n = 5. *$p$ <0.05; **$p$ <0.01, ***N.S.

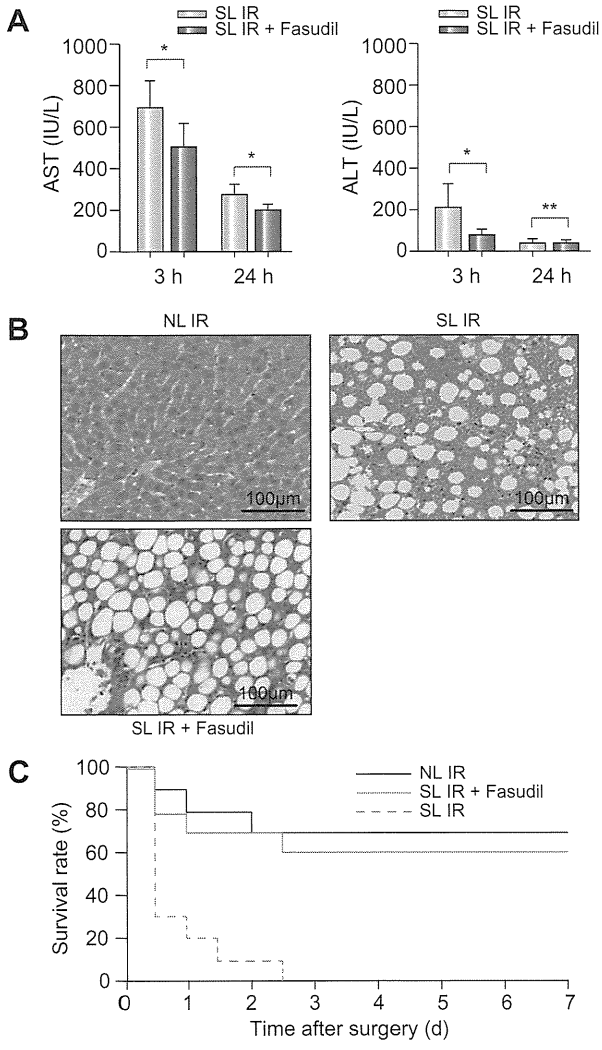


**Fig. 6. Influence of IR in rats with SL.** Rats with NL or SL were treated with IR. A fraction of the SL group received fasudil (10 mg/kg) 30 min before IR. (A) Serum levels of AST and ALT in rats with SL after 30 min of ischemia followed by 3 and 24 h of reperfusion. Average values (SD) for individual groups are shown; for all groups, n = 5. $^{*}p$ <0.05, $^{**}$N.S. (B) Histological examination of NL and SL after 45 min of ischemia followed by 24 h of reperfusion. Liver specimens from untreated rats with SL showed severe fat accumulation, distortion of architecture, sinusoidal congestion, and extensive areas of coagulative necrosis. Liver specimens from the group that received fasudil similarly showed severe fat accumulation but had a nearly normal hepatic structure and minimal sinusoidal enlargement in the hepatic lobule center compared with the untreated SL. Representative H&E-stained liver sections. (C) The survival rates of rats with NL or SL that underwent 45 min of ischemia. Although the survival rate of the SL group was significantly lower than that of the NL group ($p$ <0.01), fasudil treatment significantly improved the survival rate of the SL group ($p$ <0.01), n = 10.

ment with fasudil significantly improved the survival rate of rats with SL after IR ($p$ <0.01; Fig. 6C).

## Discussion

The SL is known to be vulnerable to IR compared with the NL. The present study is the first report to provide evidence of the effect of Rho/ROCK signaling activation in HSCs on the increased susceptibility of SL to IR injury in rats. The present results showed that the activation of HSCs in SL was associated with the upregulation of ROCK2 and that the enhanced activation of ROCK2 was involved in the induction of IR injury in SL. The intra-abdominal infusion of fasudil, a specific inhibitor of ROCK, significantly alleviated IR injury in SL.

ROCK is a downstream effector of the small GTPase Rho involved in the regulation of cytoskeletal rearrangements and cell migration. ROCK is involved in the contraction of activated HSCs, which play an important role in regulating hepatic microcirculation. Intrahepatic upregulation of ROCK contributes to increased intrahepatic resistance in cirrhotic rats and to an increased sensitivity of cirrhotic livers to vasoconstrictors [24].

In the current study, HSCs-SL showed greater stress fiber formation and overexpression of ROCK compared with NL. The contractility of the HSCs and the phosphorylation of MLC in the HSCs were significantly enhanced in SL compared with NL. These results indicated a significant activation of the HSCs-SL compared with the HSCs-NL. There have been few studies using HSCs-SL. However, liver biopsy specimens from SL and nonalcoholic steatohepatitis showed the presence of activated HSCs, identified immunohistologically using a specific monoclonal antibody to detect cytoplasmic α-smooth muscle actin, which is not present in quiescent cells. These findings revealed a correlation between the degree of HSC activation and hepatic fibrosis, and the study of these specimens suggested a trend toward increased HSC activation with increasing fat accumulation, although this lacked statistical significance [15–17]. The hepatic expression of ROCK has been shown to be elevated in livers from cirrhotic rats and patients with alcohol-induced cirrhosis, and intrahepatic upregulation of ROCK contributes to portal hypertension via an increase in hepatic vascular resistance [24]. These results indicate that the activation of HSCs may be related to the overexpression of ROCK.

In our previous report using normal rat livers, the IR-induced impairment of sinusoidal microcirculation resulted, in part, from the contraction of HSCs, and Y-27632, a specific ROCK inhibitor, suppressed the IR-induced microcirculatory disturbance by promoting the relaxation of HSCs [9].

In the present study, the portal perfusion pressure was significantly increased in SL compared with NL. The perfusion pressure in SL was further increased after IR, and fasudil significantly suppressed this pressure increase. Serum ET-1 concentration was also significantly elevated after IR, and the increase in ET-1 concentration was suppressed by the administration of fasudil. These findings indicate that fasudil attenuates microvascular injury following ischemia reperfusion in SL. ET-1, which activates the Rho/ROCK pathway and elevates portal pressure via contraction of HSCs, was used as an alternative marker for IR injury in our *in vitro* studies (including a collagen gel contraction assay and measurement of MLC and cofilin phosphorylation in HSCs). This was done because it was extremely difficult to isolate HSCs from rats with SL undergoing IR owing to insufficient perfusion of pronase and collagenase, and even when successful, the isolated HSCs showed very low viability for use in further *in vitro* studies.

The contractility of the HSCs and the phosphorylation of MLC and cofilin were significantly enhanced by ET-1 in the HSCs-SL, and fasudil attenuated these effects. Furthermore, fasudil prolonged the survival of rats with SL undergoing IR and attenuated

sinusoidal congestion and hepatocyte necrosis. These results indicate that fasudil, a specific ROCK inhibitor, suppresses IR-induced liver injury by ameliorating the hemodynamic disturbance through the modulation of Rho signaling in SL, which is more vulnerable to IR than NL.

Fasudil was used as a ROCK inhibitor in the present study based on the clinical application of the inhibitor for the release of cerebral vasospasm after subarachnoid hemorrhage [25]. Fasudil was administered at a dose of 10 mg/kg by intraperitoneal injection before IR because the area under the serum fasudil concentration curve for rats after the intraperitoneal injection of the inhibitor (10 mg/kg) was 4490 ng h/ml, which was almost compatible or slightly higher than that of fasudil in humans [26]. The use of fasudil may be a new therapeutic strategy to prevent hepatic IR injury.

The results of the current study indicated that the effect of fasudil on the contractility of HSCs-SL was mediated by the direct inhibition of ROCK, and independent of the NO effect in HSCs. Anegawa *et al.* reported that in a rat model of secondary biliary cirrhosis bile duct ligation, ROCK activation with resultant eNOS activation was substantially involved in the pathogenesis of portal hypertension. Moreover, fasudil significantly suppressed ROCK activity and increased eNOS phosphorylation through a reduction of the binding of serine/threonine Akt to ROCK and an increase of the binding of Akt to eNOS [27]. The improvement of hepatic hemodynamics by fasudil has been shown to be mediated by an enhancement of NO production by sinusoidal endothelial cells (SECs), rather than by direct inhibition of Rho-kinase in HSCs. Our result was not compatible with Anegawa's report. This may be due to differences in the experimental model used. We used a collagen gel contraction assay to show that the effect of fasudil on the contractility of HSCs-SL was mediated by direct inhibition of ROCK, while in the study by Anegawa *et al.*, a bile duct ligation-induced secondary biliary cirrhosis model revealed that the hemodynamic effects of the *in vivo* administration of fasudil were associated with the production of NO by SECs, and not by direct inhibition of ROCK. The relationship between SL and NO synthesis remains to be elucidated, and further investigation is necessary. In addition, ROCK inhibitors have been reported to improve the VLDL transport functions of hepatocytes in SL, which might be one of the mechanisms underlying their protective effect against IR injury [28].

In summary, activation of Rho/ROCK signaling in HSCs-SL is associated with an increased susceptibility to IR injury. Inhibition of ROCK attenuates the activation of the HSCs-SL and improves IR injury in rats with liver steatosis.

## Acknowledgments

The authors thank Asahi Kasei Co., Tokyo, Japan, for providing fasudil. This work was supported in part by a Grant-in-Aid for Scientific Research (KAKENHI 21591748 [to H.T.]) from the Ministry of Education, Science, Sports, and Culture of Japan.

## Conflict of interest

The authors who have taken part in this study declared that they do not have anything to disclose regarding funding or conflict of interest with respect to this manuscript.

## Supplementary data

Supplementary data associated with this article can be found, in the online version, at doi:10.1016/j.jhep.2011.04.029.

## References

[1] McCormack L, Petrowsky H, Jochum W, Furrer K, Clavien PA. Hepatic steatosis is a risk factor for postoperative complications after major hepatectomy: a matched case-control study. Ann Surg 2007;245:923–930.
[2] Gomez D, Malik HZ, Bonney GK, Wong V, Toogood GJ, Lodge JP, et al. Steatosis predicts postoperative morbidity following hepatic resection for colorectal metastasis. Br J Surg 2007;94:1395–1402.
[3] Trevisani F, Colantoni A, Caraceni P, Van Thiel DH. The use of donor fatty liver for liver transplantation: a challenge or a quagmire? J Hepatol 1996;24:114–121.
[4] Hui AM, Kawasaki S, Makuuchi M, Nakayama J, Ikegami T, Miyagawa S. Liver injury following normothermic ischemia in steatotic rat liver. Hepatology 1994;20:1287–1293.
[5] Wada K, Fujimoto K, Fujikawa Y, Shibayama Y, Mitsui H, Nakata K. Sinusoidal stenosis as the cause of portal hypertension in choline deficient diet induced fatty cirrhosis of the rat liver. Acta Pathol Jpn 1974;24:207–217.
[6] Caraceni P, Ryu HS, Subbotin V, De Maria N, Colantoni A, Roberts L, et al. Rat hepatocytes isolated from alcohol-induced fatty liver have an increased sensitivity to anoxic injury. Hepatology 1997;25:943–949.
[7] Seifalian AM, Chidambaram V, Rolles K, Davidson BR. In vivo demonstration of impaired microcirculation in steatotic human liver grafts. Liver Transpl Surg 1998;4:71–77.
[8] Zhang JX, Bauer M, Clemens MG. Vessel- and target cell-specific actions of endothelin-1 and endothelin-3 in rat liver. Am J Physiol 1995;269.
[9] Mizunuma K, Ohdan H, Tashiro H, Fudaba Y, Ito H, Asahara T. Prevention of ischemia-reperfusion-induced hepatic microcirculatory disruption by inhibiting stellate cell contraction using rock inhibitor. Transplantation 2003;75:579–586.
[10] Ankoma-Sey V, Wang Y, Dai Z. Hypoxic stimulation of vascular endothelial growth factor expression in activated rat hepatic stellate cells. Hepatology 2000;31:141–148.
[11] Hirose M, Ishizaki T, Watanabe N, Uehata M, Kranenburg O, Moolenaar WH, et al. Molecular dissection of the Rho-associated protein kinase (p160ROCK)-regulated neurite remodeling in neuroblastoma N1E–115 cells. J Cell Biol 1998;141:1625–1636.
[12] Maekawa M, Ishizaki T, Boku S, Watanabe N, Fujita A, Iwamatsu A, et al. Signaling from Rho to the actin cytoskeleton through protein kinases ROCK and LIM-kinase. Science 1999;285:895–898.
[13] Kimura K, Ito M, Amano M, Chihara K, Fukata Y, Nakafuku M, et al. Regulation of myosin phosphatase by Rho and Rho-associated kinase (Rho-kinase). Science 1996;273:245–248.
[14] Amano M, Chihara K, Kimura K, Fukata Y, Nakamura N, Matsuura Y, et al. Formation of actin stress fibers and focal adhesions enhanced by Rho-kinase. Science 1997;275:1308–1311.
[15] DeLeve LD, Wang X, Kanel GC, Atkinson RD, McCuskey RS. Prevention of hepatic fibrosis in a murine model of metabolic syndrome with nonalcoholic steatohepatitis. Am J Pathol 2008;173:993–1001.
[16] Washington K, Wright K, Shyr Y, Hunter EB, Olson S, Raiford DS. Hepatic stellate cell activation in nonalcoholic steatohepatitis and fatty liver. Hum Pathol 2000;31:822–828.
[17] Reeves HL, Burt AD, Wood S, Day CP. Hepatic stellate cell activation occurs in the absence of hepatitis in alcoholic liver disease and correlates with the severity of steatosis. J Hepatol 1996;25:677–683.
[18] Elinav E, Ali M, Bruck R, Brazowski E, Phillips A, Shapira Y, et al. Competitive inhibition of leptin signaling results in amelioration of liver fibrosis through modulation of stellate cell function. Hepatology 2009;49:278–286.
[19] Sohail MA, Hashmi AZ, Hakim W, Watanabe A, Zipprich A, Groszmann RJ, et al. Adenosine induces loss of actin stress fibers and inhibits contraction in hepatic stellate cells via Rho inhibition. Hepatology 2009;49:185–194.
[20] Ushitora Y, Tashiro H, Ogawa T, Tanimoto Y, Kuroda S, Kobayashi T, et al. Suppression of hepatocellular carcinoma recurrence after rat liver transplantation by FTY720, a sphingosine-1-phosphate analog. Transplantation 2009;88:980–986.
[21] Ikeda H, Nagashima K, Yanase M, Tomiya T, Arai M, Inoue Y, et al. Sphingosine 1-phosphate enhances portal pressure in isolated perfused liver via S1P2 with Rho activation. Biochem Biophys Res Commun 2004;320:754–759.

[22] van der Heijden M, Versteilen AM, Sipkema P, van Nieuw Amerongen GP, Musters RJ, Groeneveld AB. Rho-kinase-dependent F-actin rearrangement is involved in the inhibition of PI3-kinase/Akt during ischemia-reperfusion-induced endothelial cell apoptosis. Apoptosis 2008;13:404–412.
[23] Selzner M, Rudiger HA, Sindram D, Madden J, Clavien PA. Mechanisms of ischemic injury are different in the steatotic and normal rat liver. Hepatology 2000;32:1280–1288.
[24] Zhou Q, Hennenberg M, Trebicka J, Jochem K, Leifeld L, Biecker E, et al. Intrahepatic upregulation of RhoA and Rho-kinase signalling contributes to increased hepatic vascular resistance in rats with secondary biliary cirrhosis. Gut 2006;55:1296–1305.
[25] Suzuki Y, Shibuya M, Satoh S, Sugimoto Y, Takakura K. A postmarketing surveillance study of fasudil treatment after aneurysmal subarachnoid hemorrhage. Surg Neurol 2007;68:126–131.
[26] Satoh S, Utsunomiya T, Tsurui K, Kobayashi T, Ikegaki I, Sasaki Y, et al. Pharmacological profile of hydroxy fasudil as a selective rho kinase inhibitor on ischemic brain damage. Life Sci 2001;69:1441–1453.
[27] Anegawa G, Kawanaka H, Yoshida D, Konishi K, Yamaguchi S, Kinjo N, et al. Defective endothelial nitric oxide synthase signaling is mediated by rho-kinase activation in rats with secondary biliary cirrhosis. Hepatology 2008;47:966–977.
[28] Kitamura K, Tada S, Nakamoto N, Toda K, Horikawa H, Kurita S, et al. Rho/Rho kinase is a key enzyme system involved in the angiotensin II signaling pathway of liver fibrosis and steatosis. J Gastroenterol Hepatol 2007;22:2022–2033.

# Suppression of immune responses by nonimmunogenic oligodeoxynucleotides with high affinity for high-mobility group box proteins (HMGBs)

Hideyuki Yanai[a,b,1], Shiho Chiba[a,1], Tatsuma Ban[a,1], Yukana Nakaima[a], Takashi Onoe[c], Kenya Honda[a,d], Hideki Ohdan[c], and Tadatsugu Taniguchi[a,b,2]

[a]Department of Immunology, Graduate School of Medicine and Faculty of Medicine, University of Tokyo, Tokyo 113-0033, Japan; [b]Core Research for Evolution Science and Technology, Japan Science and Technology Agency, Tokyo 102-0075, Japan; [c]Department of Surgery, Division of Frontier Medical Science, Graduate School of Biomedical Sciences, Hiroshima University, Hiroshima 734-8551, Japan; and [d]Precursory Research for Embryonic Science and Technology, Japan Science and Technology Agency, Saitama 332-0012, Japan

Contributed by Tadatsugu Taniguchi, May 27, 2011 (sent for review May 13, 2011)

**The activation of innate immune responses by nucleic acids is central to the generation of host responses against pathogens; however, nucleic acids can also trigger the development and/or exacerbation of pathogenic responses such as autoimmunity. We previously demonstrated that the selective activation of nucleic acid-sensing cytosolic and Toll-like receptors is contingent on the promiscuous sensing of nucleic acids by high-mobility group box proteins (HMGBs). From this, we reasoned that nonimmunogenic nucleotides with high-affinity HMGB binding may function as suppressing agents for HMGB-mediated diseases, particularly those initiated and/or exacerbated by nucleic acids. Here we characterize an array of HMGB-binding, nonimmunogenic oligodeoxynucleotides (ni-ODNs). Interestingly, we find that binding affinity is rather independent of nucleotide sequence, but is instead dependent on length and structure of the deoxyribose backbone. We further show that these ni-ODNs can strongly suppress the activation of innate immune responses induced by both classes of nucleic acid-sensing receptors. We also provide evidence for the suppressive effect of an ni-ODN, termed ISM ODN, on the induction of adaptive immune responses and in mouse models of sepsis and autoimmunity. We discuss our findings in relation to the critical role of HMGBs in initiating immune responses and the possible use of these ni-ODNs in therapeutic interventions.**

pattern recognition receptors | retinoic acid-inducible gene I-like receptor | experimental autoimmune encephalomyelitis

The innate immune system is integral to the protection of the host against invading pathogens by providing immediate defense and the subsequent activation of the adaptive immune system. Pattern recognition receptors (PRRs) are germ line-encoded receptors that recognize conserved pathogen-associated molecular patterns (PAMPs) and potently activate cells of the innate immune system (1, 2). The protective role of PRRs against infectious microbial pathogens via the induction of adaptive immunity has been unequivocally demonstrated; however, the activation of these receptors may also result in eliciting harmful immune responses such as life-threatening inflammation and autoimmunity (3, 4). During microbial infection or tissue damage, DNA and RNA potently activate the innate and subsequent adaptive immune responses. In mammals, the transmembrane PRR Toll-like receptor (TLR)3, TLR7, and TLR9, respectively, recognize double-stranded RNA, single-stranded and short double-stranded RNAs, and hypomethylated DNA, whereas retinoic acid-inducible gene I (RIG-I)-like receptors, namely RIG-I and melanoma differentiation-associated gene 5 (MDA5), are best known as RNA-sensing receptors in the cytosol, but more recently have been shown to also participate in the cytosolic DNA-sensing system (5–8). In addition, cytosolic DNA-sensing receptors, which include DNA-dependent activator of IFN regulatory factors (IRFs) (DAI), absent in melanoma 2 (AIM2), among others, have been identified (9, 10). The hallmark of the innate immune responses activated by these receptors is the induction of type I IFNs, proinflammatory cytokines, and chemokines, except for AIM2, which induces the inflammasome (6, 10).

We showed previously that high-mobility group box proteins (HMGB1, 2, and 3) are essential for triggering all nucleic acid receptor-mediated innate immune responses (11). Indeed, HMGBs bind to various immunogenic nucleic acids in vitro, and cells in which the expression of HMGBs is suppressed exhibit a profound defect in their ability to evoke innate immune responses, indicating a hierarchy in the nucleic acid-mediated activation of immune responses wherein the selective activation of nucleic acid-sensing receptors is contingent on the more promiscuous sensing of nucleic acids by HMGBs. In addition, HMGB1 is secreted by innate immune cells in response to PAMPs and released by injured or dying cells, and transmits signals to the cell interior via the activation of receptors that include TLR4, thereby occupying a crucial role in the pathogenesis of both sterile and infectious inflammations (12–14). In this context, numerous antagonists that neutralize HMGB1 in preclinical disease models have supported the role of HMGB1 in regulating innate and adaptive immune responses in health and during inflammatory diseases such as arthritis, sterile ischemia/reperfusion injury, cancer, and infection (15, 16). Thus, selectively targeting HMGB1 and its family members may be of clinical use and could provide key insights into the pathogenesis of various inflammation-associated diseases.

In view of our previous findings that HMGBs bind nucleic acids promiscuously, we searched for nonimmunogenic oligodeoxynucleotides (ni-ODNs) showing high-affinity HMGB binding with the rationale that such nucleotides may effectively suppress HMGB-associated diseases initiated and/or exacerbated by nucleic acids. Here we introduce an array of ni-ODNs that can strongly bind to HMGBs, which we find depends on their length and phosphorothioate deoxyribose backbone. We also show an inhibitory effect of an ni-ODN in the induction of adaptive immune responses as well as in animal disease models associated with HMGBs, and discuss the significance of our findings from a therapeutic point of view.

## Results

**Generation of ni-ODNs with High-Affinity Binding to HMGBs.** On the basis of our previous finding that the TLR9 agonist CpG-B ODN shows a markedly high affinity with HMGBs (11), we rational-

Author contributions: H.Y., S.C., T.B., K.H., H.O., and T.T. designed research; H.Y., S.C., T.B., Y.N., and T.O. performed research; T.O. and H.O. contributed new reagents/analytic tools; H.Y., S.C., T.B., and T.T. analyzed data; and H.Y., S.C., T.B., K.H., and T.T. wrote the paper.

The authors declare no conflict of interest.

[1]H.Y., S.C., and T.B. contributed equally to this work.

[2]To whom correspondence should be addressed. E-mail: tada@m.u-tokyo.ac.jp.

This article contains supporting information online at www.pnas.org/lookup/suppl/doi:10.1073/pnas.1108535108/-/DCSupplemental.

ized that analogs without the CpG motif may also show similar if not higher affinities with HMGBs but, unlike CpG-B ODN, which activates TLR9 (5), will be nonimmunogenic (17). Thus, we generated ODNs carrying GpG or GpC in lieu of the CpG dinucleotide sequence of CpG-B ODN (Fig. S1*A*), respectively termed ISM ODN and ISR ODN, and then examined their interaction with HMGBs with these ODNs by competitive pull-down assay: In this assay, inhibition of the precipitation of a recombinant HMGB protein by biotin-conjugated CpG-B ODN was monitored by increasing the amounts of unconjugated ODN of interest (11). As expected, the precipitation of HMGB1 was inhibited by unconjugated CpG-B ODN in a dose-dependent manner, whereas ISM and ISR ODNs also showed inhibition in this assay (Fig. 1*A*). Among the three ODNs examined, the half-maximal inhibitory concentration ($IC_{50}$) was lowest for ISM ODN, suggesting that ISM ODN has the highest affinity with HMGB1 (Fig. 1*A*). Unlike CpG-B ODN, ISM and ISR ODNs were inert in evoking innate immune responses on the basis of cytokine induction in dendritic cells (DCs) (Fig. S1*B*).

Because these ODNs all have a phosphorothioate backbone instead of the usual phosphodiester backbone (11), we next asked whether the nature of the sugar backbone would affect ODN affinity with HMGB1 by generating an ISM ODN with a natural phosphodiester bond, termed PD-ISM ODN. When PD-ISM ODN was subjected to the pull-down assay, the inhibition of HMGB1–CpG-B ODN interaction was not observed, indicating that the phosphorothioate backbone is a critical element for ODN binding to HMGB1 (Fig. 1*B*). However, because the inhibition of HMGB1 precipitation by a base-free phosphorothioate deoxyribose homopolymer, termed PS (18), is far weaker than the inhibition by CpG-B ODN and ISM and ISR ODNs of identical length, it is clear that the bases also contribute to HMGB1 binding (Fig. 1*B*).

The above observations prompted us to examine whether the base sequence and length of ODNs affect their binding to HMGB1 by generating various lengths of poly(dA) with the phosphorothioate backbone (Fig. S1*C*). As shown in Fig. 1*C*, 20-mer poly (dA) (A20 ODN) inhibited the binding of HMGB1 to CpG-B ODN, but the inhibition was much weaker for 15-mer poly(dA) (A15 ODN), whereas 10- and 5-mer poly(dA) (A10 and A5 ODNs, respectively) failed to inhibit the CpG-B ODN–HMGB1 interaction entirely. Essentially the same observations were made when poly(dC) ODNs (C20, C15, C10, and C5 ODNs) were similarly examined (Fig. S1*D*). These observations thus identify three critical elements of ODNs for their high-affinity binding to HMGB1, namely ODN phosphorothioate backbone and length and, albeit to a lesser extent, base sequence. Finally, we also found that HMGB1, HMGB2, and HMGB3 were all bound directly to ISM ODN (Fig. S1*E*). Collectively, these results are consistent with our previous finding of promiscuous binding of HMGBs (11) and demonstrate that even ni-ODNs can bind HMGBs with high affinity, provided that they have the characteristics defined above.

**Suppressive Effect of ISM ODN on Nucleic Acid-Mediated Immune Responses.** We next examined whether ISM ODN, which shows the highest binding affinity with HMGBs, suppresses nucleic acid-mediated innate immune responses. As shown in Fig. 2*A*, mouse embryonic fibroblasts (MEFs) pretreated with ISM ODN and subsequently stimulated with poly(dA-dT)·poly(dT-dA) (B-DNA) (19) or poly(I:C) showed markedly suppressed mRNA induction of type I IFNs, IL-6, and RANTES genes compared with mock-treated MEFs; as expected, ISM ODN strongly interferes with the binding of HMGB1 to B-DNA or poly(I:C) (Fig. S2*A*). On the other hand, the mRNA induction of the same genes by lipopolysaccharide (LPS) stimulation remained unaffected (Fig. S2*B*). To examine the correlation between HMGB binding affinity and the suppressive effect of the above ODNs, we compared ISM ODN with CpG-B ODN, ISR ODN, PS, and PD-ISM ODN for their suppressive effect on cytosolic nucleic acid stimulations in MEFs. As shown in Fig. 2*B*, mRNA induction of the cytokine genes was also strongly suppressed by CpG-B or ISR ODNs, albeit less effectively than ISM ODN. On the other hand, the suppressive effect was very weak, if at all, for PS and PD-ISM ODN. Essentially the same observation was made for the induction of IFN-β and IL-6 secretion by ELISA (Fig. S2 *C* and *D*). In addition, A20 or C20 ODNs effectively suppressed IFN-β mRNA induction by B-DNA, whereas the effect diminished rather markedly as ODN length

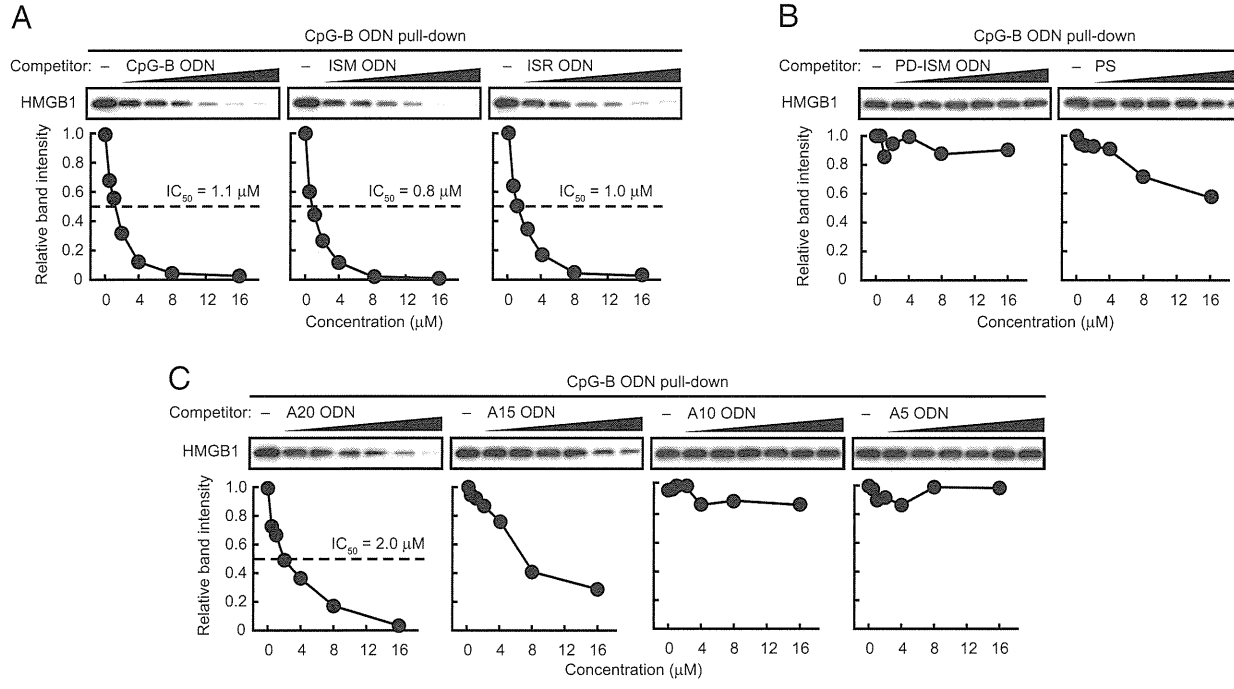


**Fig. 1.** Binding of HMGB1 to ODNs. Pull-down assay was performed using recombinant HMGB1 and biotin-conjugated CpG-B ODN in the presence of increasing amounts of unconjugated CpG-B, ISM, and ISR ODNs (*A*), PS and PD-ISM ODN (*B*), and A20, A15, A10, and A5 ODNs (*C*) (0.5, 1, 2, 4, 8, or 16 μM). The relative band intensity of precipitated HMGB1 is depicted graphically.

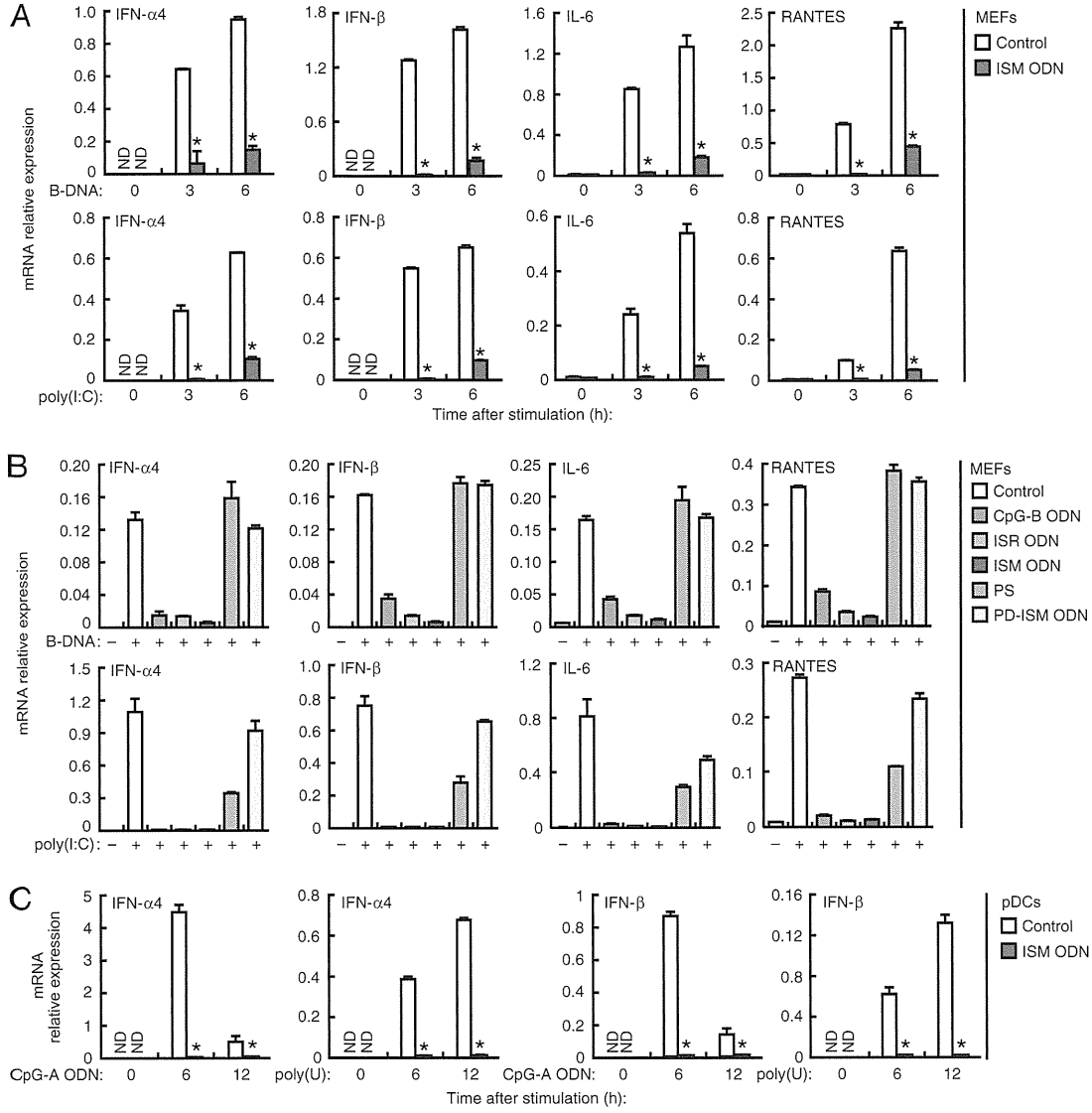


**Fig. 2.** Suppressive effect of ISM ODN on nucleic acid-mediated innate immune responses. (*A* and *B*) MEFs were left untreated (control) or pretreated with the indicated ODN (1 μM) for 1 h, and then stimulated with B-DNA (5 μg/mL) or poly(I:C) (5 μg/mL) for 3 h (*A* and *B*) or 6 h (*A*). (*C*) Bone marrow-derived pDCs were left untreated (control) or pretreated with ISM ODN for 1 h, and then stimulated with CpG-A ODN (1 μM) or poly(U) (5 μg/mL) for 6 or 12 h. Cytokine mRNA expression levels of the indicated genes were measured by quantitative RT-PCR. $^*P < 0.01$ compared with control. Data in all panels are presented as means and SD ($n = 3$). ND, not detected.

decreased (Fig. S2*E*). Thus, the suppressive effect of each ODN correlates with its binding affinity with HMGB1.

Because HMGBs are essential for both cytosolic and TLR-dependent sensing of nucleic acids (11), we next determined whether TLR responses to nucleic acids are also suppressed by ISM ODN. First, bone marrow cells were cultured in vitro with the Flt3 ligand to enrich plasmacytoid DCs (pDCs), which produce type I IFN en masse upon TLR7 or TLR9 stimulation (20), and the effect of ISM ODN was then examined. As shown in Fig. 2*C*, the mRNA induction by CpG-A ODN or poly(U), which respectively activate TLR9 and TLR7, was strongly suppressed when these cells were pretreated with ISM ODN. Consistent with this, a strong suppression by ISM ODN was also observed on the secretion of IFN-α and IFN-β by these cells (Fig. S2*F*). Similarly, when conventional DCs (cDCs), which were obtained by in vitro culture of bone marrow cells with GM-CSF, were examined for CpG-B ODN-TLR9-mediated IL-6 and TNF-α production, the ISM ODN pretreatment of the cells resulted in a strong suppression, whereas the LPS-TLR4-mediated production of the same cytokines remained unaffected (Fig. S2*G*). Taken together, these findings all support our initial rationalization that ni-ODNs with high affinity for HMGBs can selectively suppress nucleic acid-activated immune responses via cytosolic receptors or TLRs.

**Effect of ISM ODN on Cellular Delivery of and Receptor Signaling by Nucleic Acids.** To address where these ODNs exert their suppressive effect on nucleic acid-mediated innate immune responses, we first examined whether ISM ODN affects the cellular uptake of B-DNA by fluorescence microscopy. When a macrophage-like cell line, RAW264.7, was pretreated or mock-treated with ISM ODN and then transfected with rhodamine-labeled B-DNA, the B-DNA uptake in the cells was equally observed in the cytosolic fraction as spot-like shapes, suggesting that ISM ODN pretreatment does not interfere with the B-DNA uptake into the cells (Fig. 3*A* and Fig. S3*A*). Similarly, the uptake of CpG-B ODN remained unaffected by ISM ODN pretreatment (Fig. 3*B* and Fig. S3*B*). Interestingly, when rhodamine-conjugated ISM ODN was delivered into the cells, it merged with FITC-labeled dextran, an endosome/lysosome marker, as well as with LysoTracker, a lysosome marker (Fig. S3*C*); this pattern is